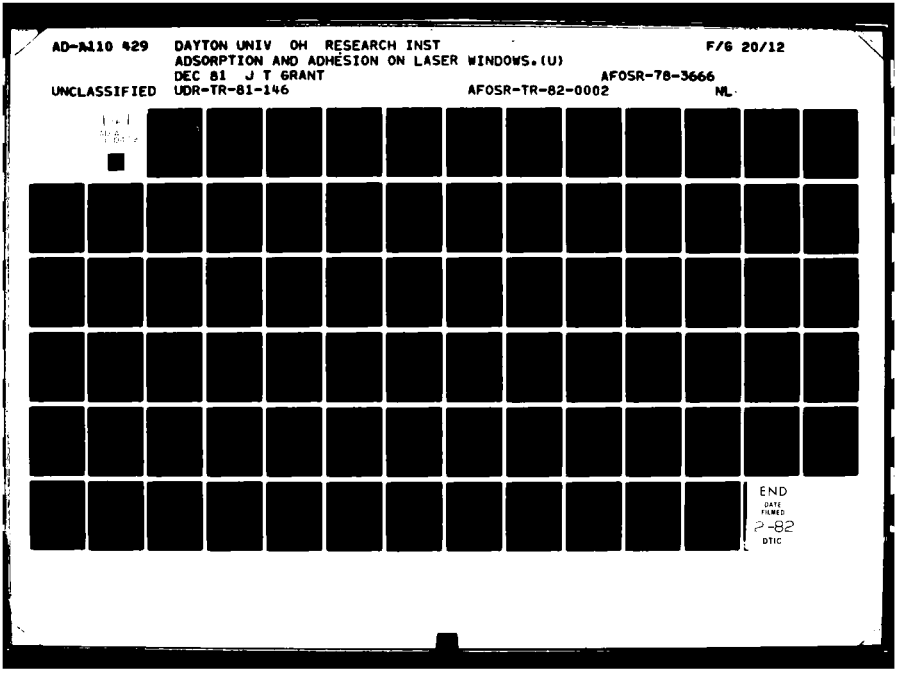
AD-A110 429
DAYTON UNIV OH RESEARCH INST
ADSORPTION AND ADHESION ON LASER WINDOWS.(U)
DEC 81 J T GRANT
F/6 20/12
AFOSR-78-3666
UNCLASSIFIED
UDR-TR-81-146
AFOSR-TR-82-0002
NL
END
DATE FILMED
2-82
DTIC

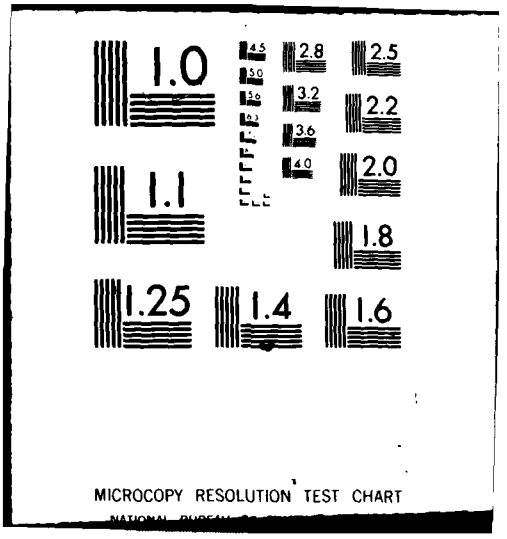
1.0
1.1
1.25
1.4
1.6
1.8
2.0
2.2
2.5
2.8
3.2
3.6
4.0
4.5
5.0
5.6
6.3
MICROCOPY RESOLUTION TEST CHART

AFOSR-TR- 82 -0002

UDR-TR-81-146

LEVEL II

12

AD A110429

ADSORPTION AND ADHESION ON LASER WINDOWS

University of Dayton Research Institute
Dayton, Ohio 45469

December 1981

FINAL TECHNICAL REPORT UDR-TR-81-146
for the Period 1 June 1978 - 30 September 1981

Approved for public release; distribution unlimited.

University of Dayton
Research Institute
Dayton, Ohio 45469

NOTICE

When Government drawings, specifications, or other data are used for any purpose other than in connection with a definitely related Government procurement operation, the United States Government thereby incurs no responsibility nor any obligation whatsoever; and the fact that the Government may have formulated, furnished, or in any way supplied the said drawings, specifications, or other data, is not to be regarded by implication or otherwise as in any manner licensing the holder or any other person or corporation, or conveying any rights or permission to manufacture use or sell any patented invention that may in any way be related thereto.

UNCLASSIFIED

SECURITY CLASSIFICATION OF THIS PAGE (When Data Entered)

REPORT DOCUMENTATION PAGE

READ INSTRUCTIONS BEFORE COMPLETING FORM

1. REPORT NUMBER: AFOSR-TR- 82 -0002	2. GOVT ACCESSION NO.: AD-A110 429
3. RECIPIENT'S CATALOG NUMBER:	
4. TITLE (and Subtitle): ADSORPTION AND ADHESION ON LASER WINDOWS	5. TYPE OF REPORT & PERIOD COVERED: Final Technical Report 1 June 1978-30 Sep 1981
	6. PERFORMING ORG. REPORT NUMBER: UDR-TR-81-146
7. AUTHOR(s): John T. Grant	8. CONTRACT OR GRANT NUMBER(s): AFOSR-78-3666
9. PERFORMING ORGANIZATION NAME AND ADDRESS: University of Dayton Research Institute, 300 College Park, Dayton, OH 45469	10. PROGRAM ELEMENT, PROJECT, TASK AREA & WORK UNIT NUMBERS: 61102F 2306/A2
11. CONTROLLING OFFICE NAME AND ADDRESS: Air Force Office of Scientific Research, Bolling Air Force Base, DC 20382	12. REPORT DATE: December 1981
	13. NUMBER OF PAGES: 84
14. MONITORING AGENCY NAME & ADDRESS (if different from Controlling Office)	15. SECURITY CLASS. (of this report): Unclassified
	15a. DECLASSIFICATION/DOWNGRADING SCHEDULE

16. DISTRIBUTION STATEMENT (of this Report)

Approved for public release; distribution unlimited.

17. DISTRIBUTION STATEMENT (of the abstract entered in Block 20, if different from Report)

18. SUPPLEMENTARY NOTES

19. KEY WORDS (Continue on reverse side if necessary and identify by block number)

Laser window	Surface analysis
Adsorption	Ion scattering spectroscopy
Calcium fluoride	Auger electron spectroscopy
Water	Electron loss spectroscopy
	X-ray photoelectron spectroscopy

20. ABSTRACT (Continue on reverse side if necessary and identify by block number)

In this program a procedure to prepare uncontaminated calcium fluoride surfaces was developed. Characterization of the chemical composition and cleanliness of selected surfaces was performed with Auger electron spectroscopy (AES) and ion scattering spectroscopy (ISS). Electron beam-induced decomposition of the calcium fluoride was observed when using typical AES electron beam parameters (5 keV, 5μA). Threshold measurements for the onset of electron beam damage showed that AES analysis could be made without significantly altering the chemical composition of the surface by rastering a 2.5 keV electron beam with a

DD FORM 1 JAN 73 1473 EDITION OF 1 NOV 65 IS OBSOLETE

UNCLASSIFIED

SECURITY CLASSIFICATION OF THIS PAGE (When Data Entered)

1 0540

20. ABSTRACT (Continued)

current density less than 0.16 mA/cm^2. The adsorption of water on clean calcium fluoride surfaces was studied using ISS. Room-temperature exposure to >10L of water resulted in a saturated surface coverage of about a 1/4 monolayer. At a surface temperature of T_{SF} = 180 K and a water pressure of 1.3 x 10^{-6} Pa, a coverage of one monolayer occurred almost instantaneously. Desorption of the adsorbed water was found to depend upon the surface temperature of the specimen prior to water exposure which suggests perhaps two different states of adsorption. The heat of adsorption of water on argon sputter cleaned calcium fluoride was determined to be 10.8 ±0.6 kcal/mole.

ABSTRACT

In this program a procedure to prepare uncontaminated calcium fluoride surfaces was developed. Characterization of the chemical composition and cleanliness of selected surfaces was performed with Auger electron spectroscopy (AES) and ion scattering spectroscopy (ISS). Electron beam-induced decomposition of the calcium fluoride was observed when using typical AES electron beam parameters (5 keV, 5 μA). Threshold measurements for the onset of electron beam damage showed that AES analysis could be made without significantly altering the chemical composition of the surface by rastering a 2.5 keV electron beam with a current density less than 0.16 mA/cm^2. The adsorption of water on clean calcium fluoride surfaces was studied using ISS. Room-temperature exposure to >10L of water resulted in a saturated surface coverage of about a 1/4 monolayer. At a surface temperature of T_{SF} = 180 K and a water pressure of 1.3×10^{-6} Pa, a coverage of one monolayer occurred almost instantaneously. Desorption of the adsorbed water was found to depend upon the surface temperature of the specimen prior to water exposure which suggests perhaps two different states of adsorption. The heat of adsorption of water on argon sputter cleaned calcium fluoride was determined to be 10.8 ±kcal/mole.

FOREWORD

This report describes the final results of a research program undertaken to study water adsorption on calcium fluoride surfaces using Auger electron spectroscopy and ion scattering spectroscopy. The program was conducted by the University of Dayton Research Institute during the period June 1978 to September 1981 under AFOSR Grant No. 78-3666. The Principal Investigators for this program were Dr. William E. Moddeman and Dr. John T. Grant. A large portion of the experimental measurements were taken by Charles L. Strecker, a Ph.D. degree candidate in the Materials Engineering Department, University of Dayton.

The author wishes to acknowledge the Surface Science Laboratory at the University of Dayton Research Institute for providing an automated data acquisition and data processing system for the ion scattering spectrometer at no cost to this program. In addition, a special note of thanks to Anne L. Testoni, for her many hours of labor in developing computer programs for analyzing the ion scattering spectra. Finally, the author acknowledges the encouragement and technical support of the following: Mr. James R. Hoenigman and Mr. Thomas N. Wittberg of the University of Dayton Research Institute; and the continued interest of Dr. William E. Moddeman, now with the Monsanto Research Corporation, Mound Facility, Miamisburg, Ohio.

TABLE OF CONTENTS

LIST OF ILLUSTRATIONS

LIST OF ILLUSTRATIONS (Continued)

LIST OF ILLUSTRATIONS (Concluded)

LIST OF TABLES

SECTION I
INTRODUCTION

1. BACKGROUND

The alkaline earth fluorides are prime candidate materials for fabricating optical components for high energy chemical lasers operating at 2.7 μm (hydrogen fluoride) and 3.8 μm (deuterium fluoride). Laser calorimetry measurements at these wavelengths have shown that present state-of-the-art calcium fluoride, the most promising of the fluorides, exhibits optical absorptivities which are an order of magnitude higher than the predicted intrinsic values.[1,2,3] This extrinsic absorption is found to be primarily associated with the surface, particularly at 2.7 μm, and is attributed to the adsorption of water on the calcium fluoride surface. In an analysis of HF laser-calorimetry results, Horrigan and Deutsch[4] estimated, from an absorptance per surface of 0.029 percent for calcium fluoride, that a water film with a thickness of about 6Å could account for the measured absorptance. This thickness is equivalent to about two monolayers of water.[5] Indeed, two monolayers of adsorbed water on a clean calcium fluoride surface would give rise to theoretical absorptances equal to or greater than the bulk values of calcium fluoride at these wavelengths.

Water vapor adsorption by calcium fluoride powders has been investigated by several workers. The earliest studies were performed by J. H. de Boer and C. J. Dippel[6,7,8] in 1933-1934 on vacuum sublimated calcium fluoride layers. According to these authors, the water monolayer is so strongly adsorbed that it cannot be desorbed by evacuation and heating without causing surface hydrolysis. The water molecules were considered to be bonded electrostatically to the outer fluorine ion layer by dipoles involving one hydrogen atom only. Amphlett[9] showed that when freshly prepared commercial calcium fluoride powders were repeatedly cycled through water adsorption-desorption

sequences with heat treatments in between, the consecutive uptake of water decreased and after a few cycles there was no further change. This suggested that some of the more energetic adsorption sites were being deactivated because of the heat treatments. The adsorption isotherms for water on fresh calcium fluoride powder showed complete reversibility. The low heat of adsorption (2-3 kcal/mole) obtained from these isotherms suggested either physical adsorption or a weak chemisorption. Hall and Tompkins[10] and Hall, Lovell and Frankelstein[11] revealed the hydrophilic nature of the calcium fluoride surface by obtaining an apparent molecular area of adsorbed water corresponding to liquid-state packing, while heats of adsorption (10-16 kcal/mole) were interpreted in terms of a hydrogen-bonding adsorption mechanism. Similar to previous work, they found that after outgassing the calcium fluoride powder at 575 K, the room temperature water vapor isotherms indicated a decrease in hydrophilic character of the surface which they attributed to surface hydrolysis. Contrary to the earlier adsorption-desorption studies, Barraclough and Hall[12,13] have since shown with infrared studies that adsorbed water molecules are capable of bonding rather strongly to alkali and alkaline earth salts; that is, while the water molecules could not be desorbed by prolonged evacuation at room temperature, they could be desorbed at 575 K without incurring a surface hydrolysis reaction. Although the infrared data did not imply a specific bonding mechanism, Barraclough and Hall theorized that adsorption occurred either through hydrogen-bonding with the surface fluorine ions, or an electrostatic interaction with surface calcium ions. Finally, a recent study of Palik, Gibson, and Holm[14] using internal-reflection spectroscopy showed that a water film composed of a thick ($\sim$12Å) physisorbed outer layer and thin ($\sim$3Å) chemisorbed inner layer was formed on the surface of a calcium fluoride trapezoid surrounded by near-saturated water vapor. The physisorbed layer could be removed by evacuation, while vacuum baking was required to remove the chemisorbed layer. The optical constants

of the adsorbed water film were found to deviate from those of bulk water suggesting that the film had an extended or open structure.

One can make two observations from the water adsorption studies just cited, which are particularly germane to the research program reported here. First and foremost is that in all of the investigations reported hitherto, except for perhaps that of Barraclough and Hall[13] and Palik, Gibson, and Holm,[14] the chemical nature and homogeneity of the calcium fluoride surface was not established prior to the adsorption studies; the calcium fluoride utilized in these studies was most often in powder form and produced in such a manner that surface contamination, particularly by OH^- ions, would be highly probable. Indeed, the results of Amphlett[9] strongly suggest the presence of pre-adsorbed surface contaminants. Secondly, the nature of the adsorption bond between the water molecule and the calcium fluoride surface are non-conclusive. Most investigators theorize hydrogen bonding of the water molecule to the calcium fluoride surface, but they are uncertain as to whether the water molecule is singly or doubly bonded to the surface, and to what extend, if any, has the surface hydrolyzed.

2. PROGRAM APPROACH

Reported here are the results of a study to establish the mechanism and kinetics of the adsorption of water on calcium fluoride. The study was divided into two phases. In the first phase, a "clean" calcium fluoride surface of known crystallographic orientation was prepared by argon ion sputter etching. Characterization of the chemical composition and cleanliness of the surface was performed with Auger electron spectroscopy (AES) and ion scattering spectroscopy (ISS). An important aspect of this phase of the program was the observation that calcium fluoride decomposed under electron beam impact when using typical AES electron beam parameters. Results of our investigation of

electron-beam decomposition of calcium fluoride surfaces using AES, electron loss spectroscopy (ELS), and X-ray photoelectron spectroscopy (XPS) are reported in Section IV. Conditions for obtaining AES spectra from calcium fluoride under which electron-beam changes have been essentially eliminated were determined and are also reported. A paper published in the November 1981 issue of the Journal of Applied Physics describing these results is provided in Appendix A.

Phase II of this study involved the investigation of water adsorption by argon sputter cleaned calcium fluoride (111) surfaces. Results were obtained using ISS and a temperature variation method for determining water isobars. These results are reported in Section VI of this report.

SECTION II
EXPERIMENTAL

1. SPECIMENS

For most of the results reported here calcium fluoride specimens were prepared from a large gain (∿1 cm) polycrystalline ingot supplied by the Raytheon Company, Research Division, Waltham, Massachusetts.[15] This material was fabricated by a fusion casting process using a carbon tetrafluoride reactive atmosphere (RAP) for purification. Calcium fluoride produced by the RAP process represents the state-of-the-art in low contamination, high quality infrared optical grade material. Specimens were made by cleaving bars cut from the ingot, thereby allowing (111) surfaces with dimensions of ∿1 cm^2 to be obtained.

Calcium fluoride specimens with (100) and (110) surfaces were prepared from single crystal rods supplied by Optivac, Inc. These rods were oriented by Laue x-ray technique to within ±1.5 degrees of the desired orientation, cut with a diamond impregnated wire saw to reduce surface damage, and polished to a scratch free finish with 1 μm Linde A powder.

2. INSTRUMENTATION

The AES and ELS studies were performed in a Varian FC12E ion-pumped stainless steel ultrahigh vacuum (UHV) system with a base pressure of 3×10^{-8} Pa. A Varian depth profiling Auger spectrometer consisting of a single-pass cylindrical mirror analyzer (Model No. 981-2707) equipped with a coaxial electron gun having a maximum electron beam energy of 10 keV and a minimum spot size of 5 μm was used to obtain the AES and ELS spectra. In Phase I, the initial AES studies were performed with an electron beam energy of 5 keV and a current density of 14 mA/cm^2 (1 μA beam rastered over 7×10^{-5} cm^2). With these beam conditions, electron beam desorption of fluorine was observed. To eliminate electron induced desorption effects, AES spectra were

later obtained using a 2.5 keV electron beam with current densities down to 0.082 mA/cm^2. This current density was achieved by rastering a 0.05 μA beam over an area of 6×10^{-4} cm^2. In order to maintain an adequate Auger signal-to-noise level at such low beam currents, a modulation voltage of 10 eV peak-to-peak was used for the lock-in amplifier reference signal for phase-sensitive detection of the Auger current. The primary electron beam was incident at 70° with respect to the specimen normal.

For the ELS study, characteristic electron energy loss spectra were obtained with beam energies of 150, 300, and 500 eV supplied by the Auger electron gun. Current densities from 40 to 120 mA/cm^2 were used in these studies. Results were recorded using the standard AC modulation technique with a peak-to-peak modulation of 1 eV. The full-width at half-maximum (FWHM) of the elastic peak was measured to be 1.2 eV. Energy losses were measured at the minima of the derivative peaks, relative to the corresponding minimum of the elastic peak.

The XPS measurements were performed in a Leybold-Heraeus system using a LH-10 XPS spectrometer and a Mg x-ray source (1253.6 eV). In addition to XPS, the vacuum system contained a quadrupole mass spectrometer for residual gas analysis (RGA). Bake-out at 425 K gave a background pressure in the low 10^{-8} Pa range.

The ion scattering spectra reported here were obtained using a 3M Model 525 ion scattering spectrometer which uses a 138° backscatter collection geometry. In this instrument, a 3M mini-beam ion gun is coaxial with a single-pass cylindrical mirror analyzer (CMA). The minimum beam diameter of the ion gun is about 130 μm. At a primary ion beam energy of 1000 eV, this beam size provided about 18 nA of target current. The specimens were mounted both at normal incidence to the ion beam and at 45° to the primary ion beam. In all of the ISS measurements, a charge neutralization system employing a heated filament was used to minimize the effects of specimen surface charging. The principles of ISS will be discussed in more detail in Part 3 of this section.

Unless otherwise specified, the ion scattering spectra were measured with a primary beam of $^3He^+$ at an energy of 1000 eV and a current density of 80 nA/cm^2. This current density was achieved by rastering a ~190 μm diameter beam over an area of 0.15 cm^2. The ISS spectra obtained were recorded digitally using a DEC LSI-11 microcomputer featuring programmable digital control of the CMA sweep parameters. This system was developed by the Surface Science Laboratory at the University of Dayton, and was provided to this program at no cost. Digital acquisition of spectra made possible the time-averaged accumulation of data over short time periods. This rapid scan technique is statistically more accurate than the single long analog scan method originally supplied with the 3M spectrometer. The digitally acquired spectra were transmitted to a DEC VAX-11/780 computer for storage and later processing utilizing an interactive computer program developed by Anne L. Testoni. Typical computer operations performed on ISS spectra included smoothing, background subtraction, and peak heights and area calculations. Raw data as well as processed spectra could be observed on a Tektronix Model 4025 graphics terminal and recorded as necessary with a Tektronix Model 4662 interactive digital plotter. A schematic of the complete automated data acquisition and processing system developed by the University of Dayton for the Surface Science Facility is shown in Appendix B.

Initial measurements were made using a static backfilling method in which the specimen chamber (ion pump off) was filled with ^3He gas to a pressure of 8×10^{-3} Pa for analysis. This is a standard technique for inert gas sputtering in most surface spectrometers. However, repeated backfills with ^3He and ^{20}Ne sputter gas caused the ion pump to release previously pumped noble gases while the static backfill method was being used for ISS analysis. In particular, neon which was used in previous analyses, outgassed from the ion pump in significant amounts to cause interference with the ^3He spectra. As a result, a Leybold-Heraeus Model TMP 220 turbomolecular pump was purchased and installed on the vacuum system, replacing the ion pump. The

turbomolecular pump permitted a dynamic flow of the desired sputter gas injected directly into the ion gun, thereby allowing the specimen chamber to be at a pressure of 1.5×10^{-6} Pa during ISS analysis for the same ion beam current used in the static backfill mode. In this manner the ion pump memory effect was eliminated.

For the water adsorption experiments, water which had been purged of all dissolved gases had to be produced. This was accomplished by constructing a valved 25 cc stainless steel reservoir into which demineralized, triply deionized water was placed. The reservoir was then cooled in a dry ice, acetone bath and evacuated for several hours to remove dissolved gases. The cleanliness of the water vapor was monitored throughout these experiments by a residual gas analyzer mounted in the ISS specimen chamber.

The specimen temperatures T_{SF} were measured by a silicon-diode sensor placed geometrically and thermally symmetric with relation to the specimen mounted on the cold stage. This diode sensor was also used to control the temperature of the cold stage by providing a sensor signal to a Lake Shore Cryotronics, Inc. temperature controller Model DRC-80C. Temperature controllability was typically ±0.5 K.

3. ION SCATTERING SPECTROSCOPIC TECHNIQUE

It is appropriate to briefly review the principles and attributes of ion scattering spectroscopy, since this technique is the primary characterization tool employed in this study.

Ion scattering spectrometry is performed by bombarding the surface of a solid with low energy (400-4000 eV) noble gas ions and measuring the backscattered ion energy through a known scattering angle. In this energy regime backscattered noble gas ions undergo single binary elastic collisions with the surface atoms. The fractional energy lost by the noble gas ions is determined from scattering kinematics to be:

$$\frac{E}{E_o} = \frac{1}{1 + \alpha^2} \left[\cos \theta + (\alpha^2 - \sin^2\theta)^{1/2}\right]^2 \qquad \alpha \geq 1 \qquad (1)$$

in which E_o is the energy of the primary noble gas ion, E is the energy of the noble gas ion after scattering through an angle θ in the laboratory coordinate system. The parameter α is the ratio of the mass of the surface atom, m_2, to that of the scattered ion, m_1. Thus, for a fixed scattering angle, and with known values of m_1 and E_o, the mass of scattering site atoms can be determined from a measurement of the energy distribution of the scattered primary ions. An example of a scattered ion energy distribution is presented in Figure 1 for 1 keV $^3He^+$ ions scattering from calcium fluoride with $\theta = 138°$. As seen from Figure 1, atoms of different mass on the surface will each produce a scattered peak in the backscattered ion energy distribution (within the mass resolution of the technique). In addition, the scattered ion energy distribution normalized with respect to E_o is substantially independent of E_o in the range from 0.1 to 5.0 keV.[16,17]

Applying the scattering formula to calcium fluoride, the fractional energy loss E/E_o for $^3He^+$ (3.016 amu) scattered from calcium and fluorine is 0.769 and 0.572, respectively. These ratios are for ions scattered through an angle of 138° in the laboratory coordinate system. With the adsorption of water on calcium fluoride, a $^3He^+$ ion backscattering peak from oxygen will occur at an energy ratio, E/E_o, of 0.514. On the other hand, it should be clear from the scattering formula above that for $\theta > 90°$ (i.e., the backscattering mode used in this work), no scattering peak will be observed for hydrogen atoms on the surface.

One of the unique features of ISS is its surface sensitivity; the sampling depth is essentially the outer one or two atomic layers of the specimen.[18,19] Primary ions that penetrate more than two layers generally are neutralized or suffer large-angle

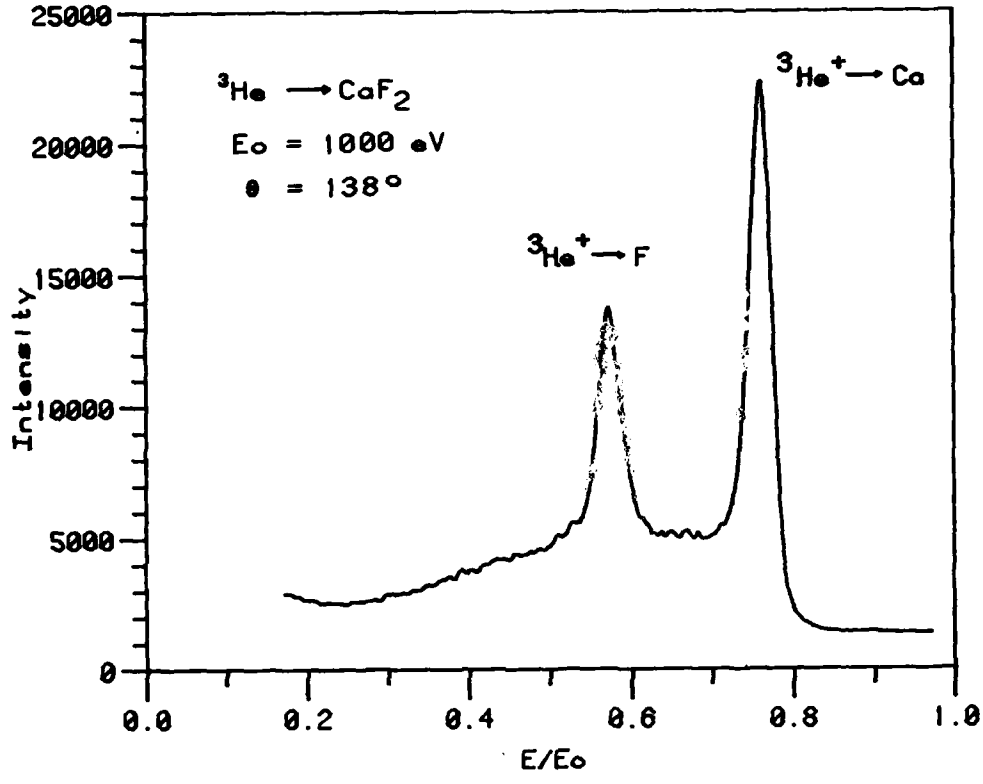

Figure 1. Energy distribution of scattered ions which indicates the prominent peaks for $^3He^+$ elastically scattered from calcium fluoride.

scattering and are not detected. Moreover, because of the classical nature of the scattering process, any addition of adsorbed atoms to the top layer of the surface leads to a screening or geometrical "shadowing" effect. As a result, the intensity of the scattering from the substrate atoms decrease with increasing coverage by adsorbed atoms or molecules. It is because of this "shadowing" effect that ISS has been successfully used as a complementary technique to AES and low energy electron diffraction (LEED) in studying orientation of adsorbed gases on single-crystal metal surface.[20,21,22,23]

SECTION III
PREPARATION OF CLEAN CALCIUM FLUORIDE SURFACES

A prerequisite for studying the adsorption of water on calcium fluoride is that the outermost atomic layer be uncontaminated. Argon sputter etching was used as a cleaning process to produce uncontaminated calcium fluoride surfaces. The cleanliness of the surface was measured to the 0.1% atomic levels with AES and ISS. These results were used to optimize the sputter etching parameters.

Calcium fluoride specimens were prepared in air and placed in the AES specimen chamber. After baking the spectrometer, the AES spectra showed sulfur, chlorine, carbon, and oxygen as the major surface contamination as shown in Figure 2. The specimens were argon ion sputter etched using an ion energy of 1 keV, a current density of 3 $\mu A/cm^2$, and a static argon backfill pressure of 6.7×10^{-3} Pa. After 20 minutes of argon ion bombardment, surfaces free of sulfur, chlorine, and carbon within AES detection limits were produced as shown in Figure 3. Surfaces prepared in this manner will be referred to as "cleaned" calcium fluoride surfaces. The persistence of an oxygen Auger signal after ion sputter etching was found consistently for all of the specimens used in this study. The source of the oxygen AES signal is from oxygen contamination in the bulk of the calcium fluoride material.[24]

Ion bombardment can cause considerable damage both structurally as well as chemically through preferential sputtering. Of particular interest were the chemical changes taking place on the calcium fluoride surface during argon sputter etching. Auger survey scans using a primary electron beam energy of 2.5 keV and a current density of 0.04 mA/cm^2 which does not produce significant decomposition of the surface (see Section IV, Part 1) were taken before, after, and at various time intervals during the argon bombardment. Because of surface

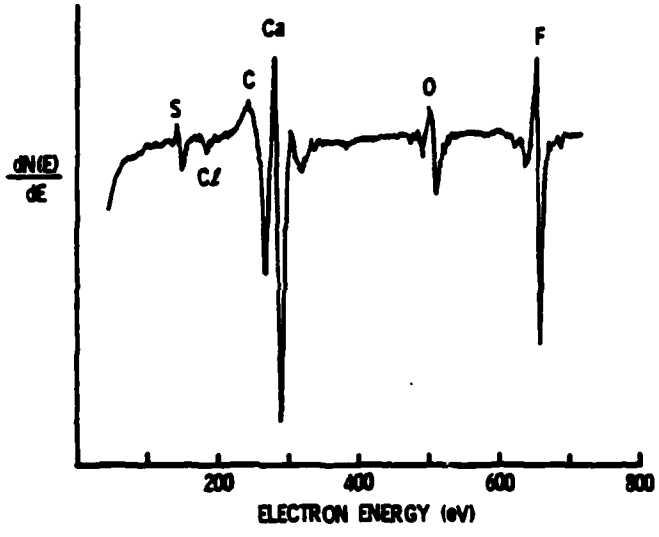

Figure 2. Auger spectrum of an unsputtered calcium fluoride surface after bake-out of UHV system.

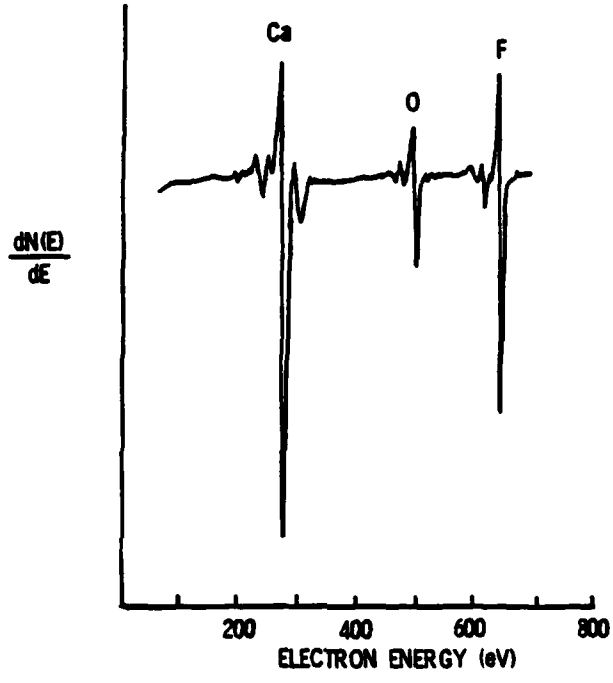

Figure 3. Auger spectrum after 20 minutes of argon sputtering using an ion energy of 1 keV, a current density of 3 $\mu A/cm^2$, and a static argon backfill pressure of 6.7×10^{-3} Pa.

charging, argon sputter etching had to be suspended during the AES analysis.

Little change in the fluorine Auger peak height was observed during the argon sputter etching process as seen in Figure 4. On the other hand, the calcium Auger peak (294 eV) increased almost two-fold. In Figure 5, the calcium Auger peaks before and after argon bombardment of the fluoride surface are shown. It is seen that the increase in the calcium Auger peaks is associated with a decrease in the carbon (273 eV) Auger peak, representing the removal of adventitious carbon from the surface.

The effect of argon ion sputter etching on calcium fluoride was also studied with ISS. In the ISS system, using dynamic sputtering as explained earlier, the specimen chamber was maintained at a pressure of 1.5×10^{-5} Pa. Sputter etching was done with an ion beam energy of 1 keV. The argon ion beam was rastered over an area of about 2 cm^2, resulting in a current density of 12 nA/cm^2. Figure 6 shows the ISS peak intensities for $^3He^+$ (1 keV) backscattered from calcium and fluorine as a function of argon sputter etch time. As with the AES analysis, after the initial cleanup of the calcium fluoride surface within the first several minutes of argon ion bombardment, little variation in either the calcium or fluorine ISS signal was observed.

It is evident, then, from the above results that argon sputter etching can be used to clean calcium fluoride surfaces without causing changes in surface stoichiometry. This is highly dependent on the choice of sputter parameters below the damage threshold. The increase in the calcium AES peak after sputtering is attributed to the removal of surface carbon which suppresses the calcium Auger signal because of the small electron escape depth of the calcium Auger electrons. Furthermore, these results indicate that an argon sputter etching time of 5 to 10 minutes at an energy of 1 keV and current density of 12 nA/cm^2 is optimum for establishing a clean calcium fluoride surface.

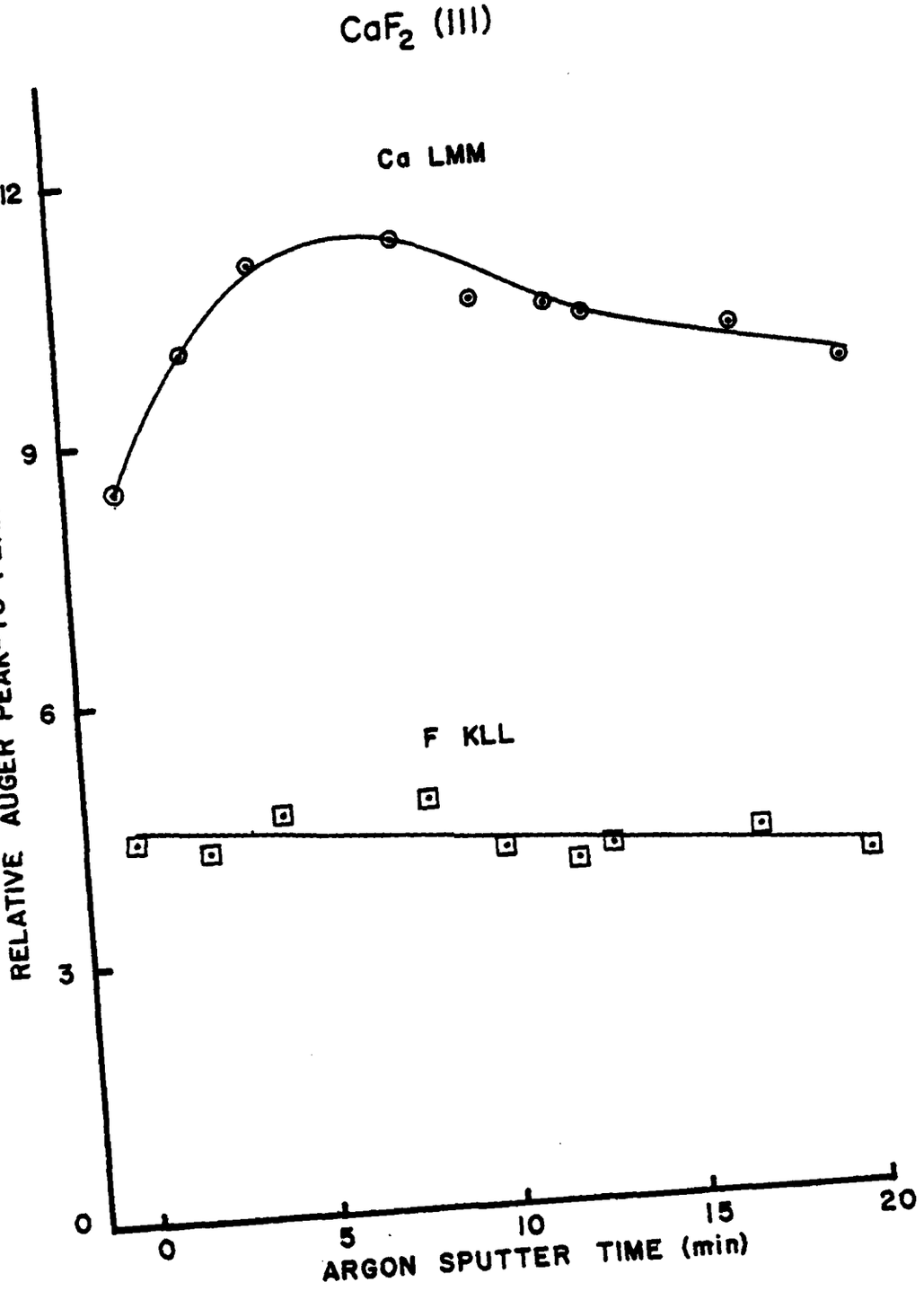

Figure 4. The peak-to-peak amplitude of calcium and fluorine Auger signal as a function of argon (1 keV, 1.4 μA) sputter etch time.

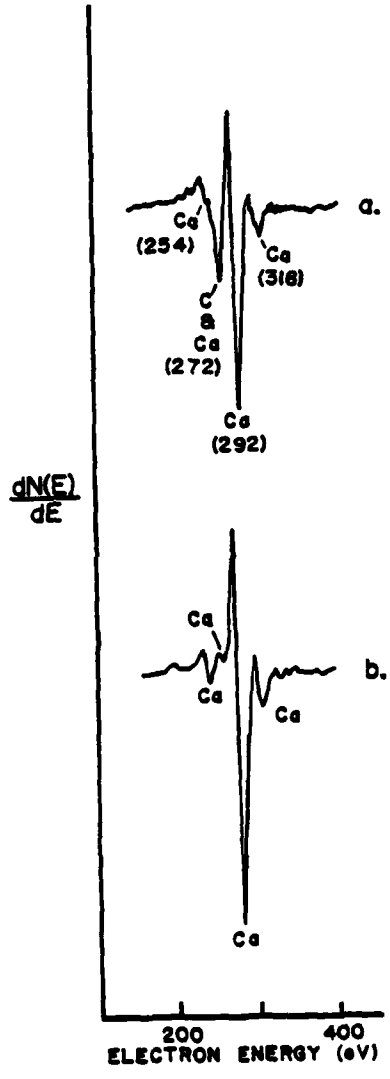

Figure 5. Auger spectrum of a calcium fluoride surface showing the calcium Auger signal: (a) before argon sputtering; (b) after 20 minutes of argon sputter etching (1 keV, 1.4 μA).

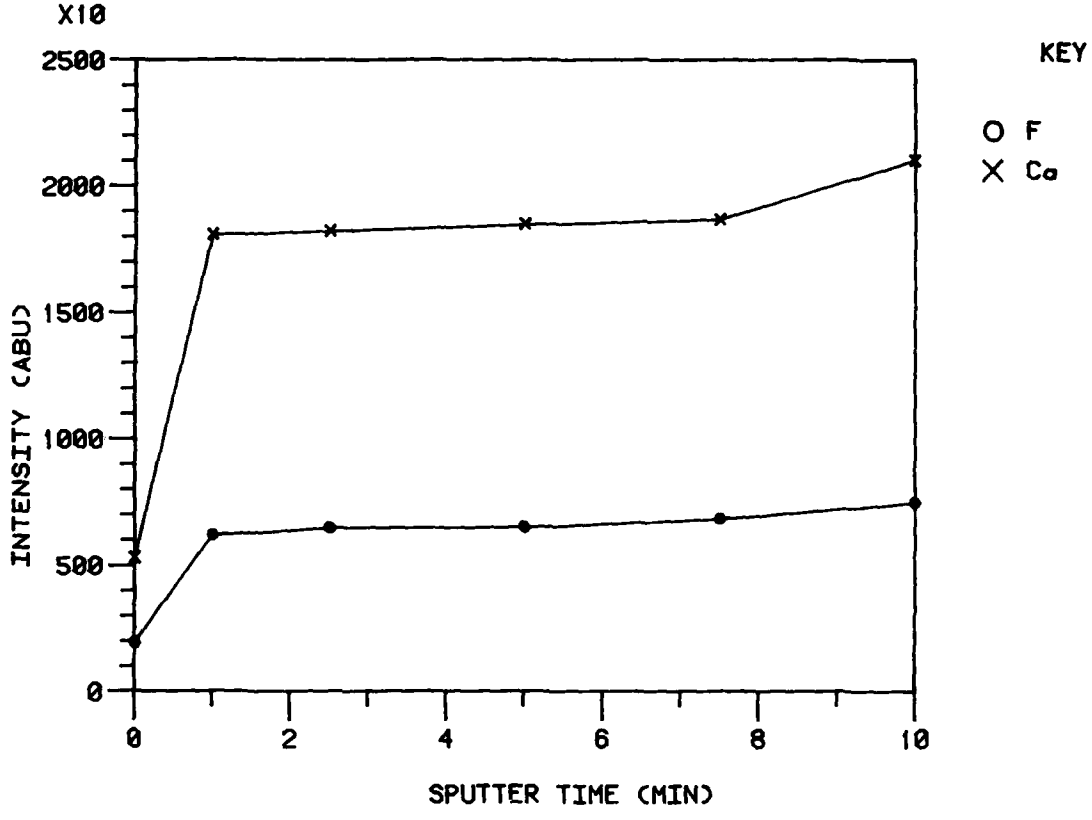

Figure 6. Variation in the calcium and fluorine ISS signal as as function of argon (1 keV, 12 nA/cm^2) sputter etch time.

SECTION IV
ELECTRON BEAM EFFECTS ON CALCIUM FLUORIDE

During the initial cleaning studies using AES, calcium fluoride had been observed to decompose under electron beam impact when using typical AES beam parameters. In this section, we report the results of our investigation of electron beam decomposition of ion bombarded calcium fluoride surfaces using AES, electron loss spectroscopy (ELS) and x-ray photoelectron spectroscopy (XPS). AES analysis showed this decomposition to be in the form of electron-induced desorption of the fluorine from the surface. In addition ELS and XPS measurements suggest that simultaneous with the desorption of fluorine from the surface, is the accumulation of calcium in a metallic-like state. Conditions for obtaining AES spectra from calcium fluoride below the damage threshold were determined and are reported.

A paper entitled "Electron-Beam-Induced Decomposition of Ion Bombarded Calcium Fluoride Surfaces" describing these results was published in the November 1981 issue of the Journal of Applied Physics (Vol. 52). A reprint of the paper is found in Appendix A.

1. AES MEASUREMENTS

The cleaned calcium fluoride surfaces were studied using the coaxial electron gun of the Auger spectrometer. At first the electron gun was observed to induce damage when operated at normal AES operating conditions. A blue glowing spot indicated the area hit by the electron beam. On removing specimens from the vacuum system, a purple coloration of the surface area impacted by the electron beam was observed. This coloration, which is indicative of the formation of F- centers, was found to be particularly pronounced for electron beams with current densities greater than 1 mA/cm^2.

Electron beam-induced changes in the AES spectra of a cleaned calcium fluoride surface are shown in Figure 7. Spectrum (a) was obtained following argon ion sputtering of the surface for 30 minutes using a 1 keV argon beam and a current density of 3 $\mu A/cm^2$. This typical spectrum persists for hours under UHV conditions without showing any significant increase in concentration of carbon or oxygen contamination, provided the specimen is not decomposed by electron bombardment during that time. Spectrum (b) was obtained after exposure of the cleaned surface to an electron beam at 2.5 keV and a current density of 15 mA/cm^2 for 20 minutes. The Auger analysis was done in both cases with a primary electron beam energy of 2.5 keV and a current density of 0.082 mA/cm^2 which does not produce significant decomposition of the surface (see end of this section). It can be seen that following electron beam decomposition the relative decrease in the fluorine Auger peak-to-peak amplitude is very pronounced (4-fold decrease).

The time dependence of the Auger signal is shown in Figure 8 using a calcium fluoride surface with a primary electron beam of 5 keV and a current density of 14 mA/cm^2. The intensity of the Auger signal was taken to be the peak-to-peak height of the dN/dE spectra. The fall-off of the fluorine Auger signal indicates that the electron beam is inducing the desorption of fluorine ions in the upper surface region of the calcium fluoride specimen. Fluorine desorption as a result of electron damage is a well known phenomenon[25] and was expected to be observed in this study.

The main Auger transitions of calcium are the $L_{2,3}MM$ transition at 293 eV and the $L_{2,3}MV$ transition at 318 eV, where the V denotes the participation of an electron from the valence band. The peak-to-peak intensity of the calcium $L_{2,3}MV$ Auger signal was observed to increase slightly during electron bombardment as shown in Figure 8. This increase in the Auger $L_{2,3}MV$ transition for calcium as a result of electron beam exposure can be attributed to a reduction in coordination number of the calcium ions in the surface region resulting from the loss of

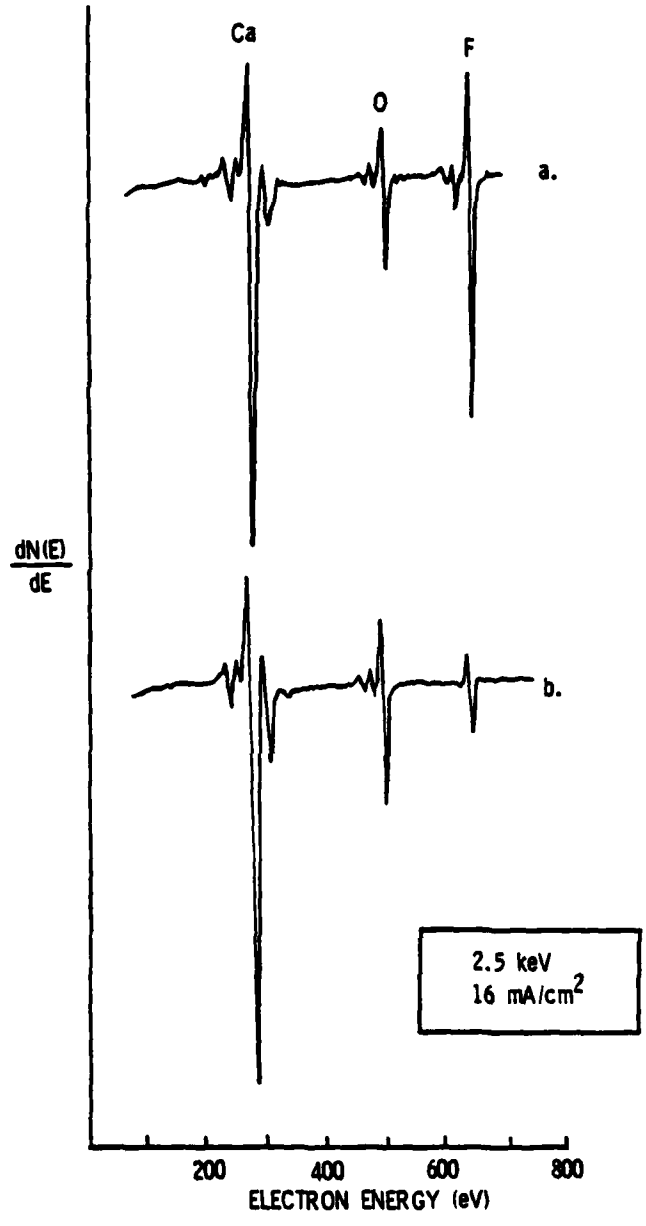

Figure 7. Auger spectrum of a cleaned calcium fluoride surface: (a) surface after sputtering; (b) after 20 minutes of electron bombardment with an energy of 2.5 keV and a current density of 16 mA/cm^2. Data were taken with a 2.5 keV electron beam with a current density of 0.082 mA/cm^2.

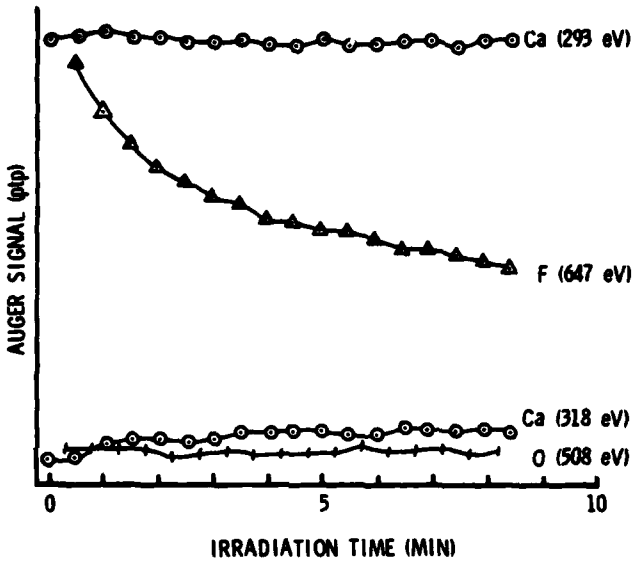

Figure 8. Time-dependent peak-to-peak amplitude of calcium, fluorine, and oxygen Auger signal from a clean calcium fluoride surface as a function of exposure time to electron bombardment. AES signal excited by a 5 keV electron beam with a current density of 14 mA/cm^2. The partial pressures of oxygen containing residual gases are less than 1×10^{-8} Pa.

fluorine, thereby increasing the number of electrons associated with the valence band. On the other hand the Auger peak-to-peak intensity of the calcium $L_{2,3}MM$ transition (293 eV) remains essentially unchanged during electron bombardment. Because the peak-to-peak intensity of the calcium $L_{2,3}MM$ Auger signal remains unchanged does not necessarily mean that the Auger current of the $L_{2,3}MM$ transition did not increase. It is well known that changes in the Auger line shapes can produce erroneous results when using peak-to-peak intensities as a measure of the detected Auger currents. This is found to be the case, for example, when performing AES depth profiling through thin films of aluminum and silicon oxides on their respective pure materials, in which energy shifts in the metal Auger transitions indicate a depletion of the metal near the interface in the peak-to-peak intensity depth profile.[26] Broadening of the calcium $L_{2,3}MM$ Auger peak may occur due to changes in the bonding of the calcium as a result of the loss of fluorine. Such broadening would correspond to a higher calcium $L_{2,3}MM$ Auger current from the specimen, even though the peak-to-peak height would not change. Indeed, the calcium 2p levels were observed to broaden substantially after prolonged electron bombardment using XPS (see Part 3 of this section).

Electron beam assisted oxygen adsorption was observed depending upon the partial pressure of oxygen containing gases (e.g. O_2, H_2O, CO and CO_2) present in the residual gas of the UHV specimen chamber. During electron beam bombardment, if the partial pressure of the oxygen containing gases is below $\sim 1 \times 10^{-8}$ Pa, the oxygen Auger signal shows no more than perhaps a small variation in intensity. On the other hand, if the partial pressure is above $\sim 5 \times 10^{-8}$ Pa, the oxygen Auger signal increases simultaneously with the decrease in the fluorine Auger signal as illustrated in Figure 9. Because of this effect, the measurements reported in this section were taken with the oxygen partial pressure less than $\sim 1 \times 10^{-8}$ Pa.

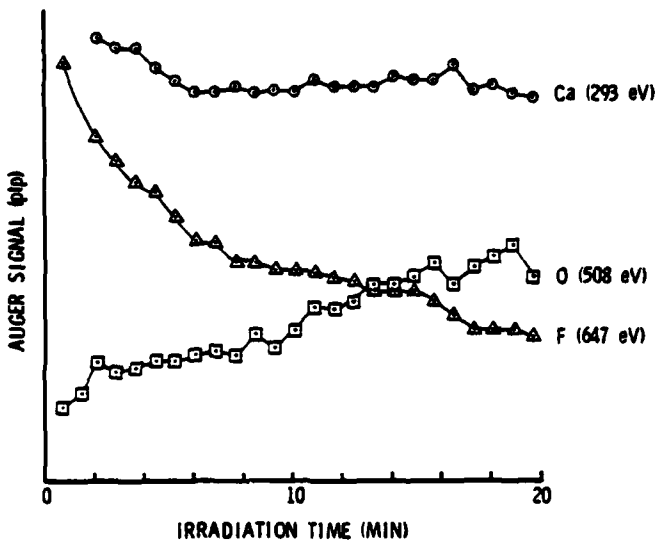

Figure 9. Time-dependent AES peak intensities from a calcium fluoride surface as a function of exposure time to electron bombardment with a 5 keV electron beam and a current density of 14 mA/cm^2. The partial pressures of oxygen containing residual gases are above 5 x 10^{-8} Pa.

In order to permit Auger analysis of the calcium fluoride surface without causing electron beam damage, a series of measurements were performed to determine the current density reshold for electron induced desorption of fluorine from the surface. Since the electron beam current was known but the beam diameter was not known, the current density was measured by rastering the beam over an area of 6×10^{-4} cm^2. The fluorine desorption rate for a cleaned calcium fluoride surface was determined for electron beam current densities of 0.082, 0.15, 1.6, 4.1 and 8.2 mA/cm^2.

The rate of fluorine desorption increased with increasing electron current density. Assuming a first order desorption process, an effective cross section for electron stimulated desorption of $\sim 7.5 \times 10^{-19}$ cm^2 was determined for a 2.5 keV electron beam from the fluorine Auger signal strength taken as a function of electron irradiation time. Using this cross section leads to a calculated damage threshold or critical electron dose, D_d, of ~ 0.21 C/cm^2, assuming a 10 percent detectable change in concentration of fluorine within the expected escape depth of 9 monolayers. This electron dose can be related to the electron beam parameters since electron dose is given by the product of current density ($amps/cm^2$) and time (sec). Hence, on the basis of the value given above for D_d, detectable damage to a calcium fluoride surface would not occur until 35 minutes for an electron current density of 0.1 mA/cm^2. Indeed, for current densities of 0.16 mA/cm^2 and below, little variation in the magnitude of the fluorine Auger signal was observed for exposures up to 20 minutes as illustrated in Figure 10.

There are two mechanisms by which an electron beam can cause a color center and the dissociation of a fluorine atom from the surface. One possible mechanism is the absorption of electrons with low energy ($\sim$2-4 eV) in the valence band leading to a chemical dissociation process analogous to the process proposed by Hersh[27] and by Pooley[28] for the formation of color centers in alkali halides. Another possible mechanism is that

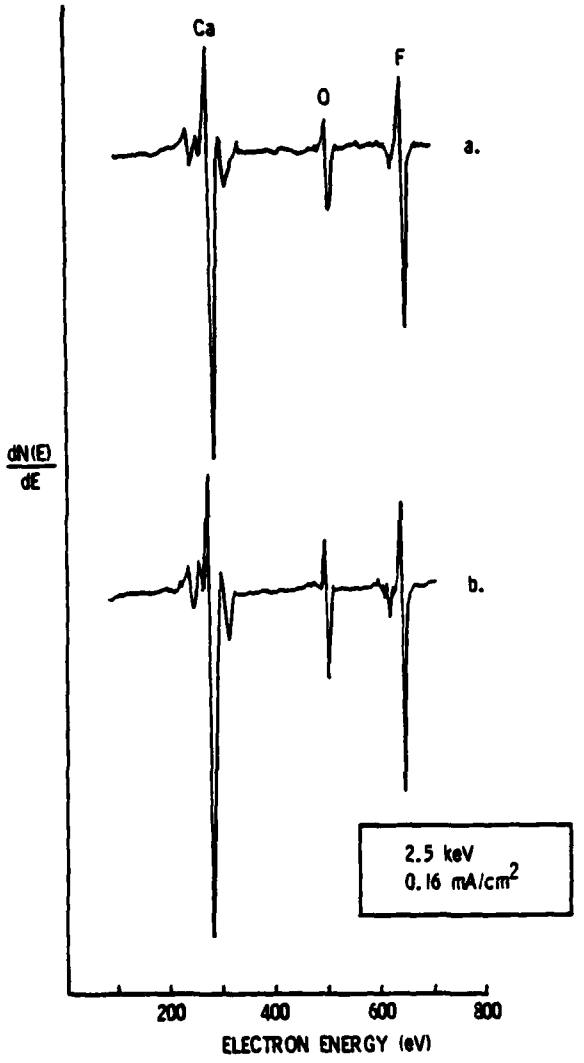

Figure 10. Auger spectrum of a clean calcium fluoride surface: (a) before electron bombardment; (b) after 20 minutes of exposure to an electron beam with an energy of 2.5 keV and a current density of 0.16 mA/cm^2.

recently proposed by Knotek and Feibelman[29] which should be applicable to ionic solids. These authors suggest that the probable path to desorption in a maximal valency ionic compound, such as calcium fluoride, is via an inter- or intra-atomic Auger decay of the core holes produced by the primary electron beam. When this decay occurs two (or even three) electrons are removed from the anions. This will make the Madelung potential, which is strongly attractive in the ground state, strongly repulsive and thus lead to desorption of neutral or positively charged anions. In the case of calcium fluoride, such a mechanism is feasible via an intra-atomic Auger transition originating from a fluorine 2s hole. However, the desorption data presented here does not clarify which mechanism is operative for the electron beam-induced desorption of fluorine from calcium fluoride.

From the Auger measurements it was noted that when a calcium fluoride surface is exposed to an electron beam with current densities greater than 0.16 mA/cm^2, a pronounced decrease in the fluorine Auger signal strength is observed. On the other hand a small increase in the calcium $L_{2,3}MV$ is observed while little change in the calcium $L_{2,3}MM$ Auger signal is noted. To characterize the chemical changes undergone by the calcium ions during electron beam bombardment, studies of electron irradiated calcium fluoride surfaces were performed using ELS and a combination of XPS and x-ray stimulated AES (XAES). The following two sub-sections describe these results.

2. ELECTRON LOSS MEASUREMENTS

Electron loss measurements of air cleaved calcium fluoride surfaces at room temperature were made using incident electron beam energies of 150, 300, and 500 eV at current densities from 40 to 120 mA/cm^2. A series of energy loss spectra taken as a function of irradiation time for an incident electron energy of 150 eV are shown in Figure 10. Loss peaks were observed at 3, 7, 11, 15, 27, and 33 eV below the elastic peak. The electron loss

spectra obtained with the 300 eV and 500 eV incident electron beams were found to be similar to those obtained in the 150 eV beam studies.

As shown in Figure 11, the cumulative effect of electron bombardment of a calcium fluoride surface produced significant changes in the energy loss spectrum. In each of the ELS spectra the two lowest energy loss peaks are enhanced in intensity with increasing irradiation time. Simultaneous with this increase, the loss peak at 15 eV is gradually obliterated.

Based on experimental loss data[30] and electronic energy band calculations,[31] reasonable assignments can be made to the observed electron loss spectra. Table I lists the energy losses of the calcium fluoride surface taken at a primary electron energy of 150 eV. Also listed in the table are the energy-loss values found from electron transmission measurements[30] and from optical measurements.[32] Further, a labeling and proposed origin for each loss peak is also given.

The strong 33 eV loss is caused by electronic transitions from the low valence bands originating mainly from the 3p Ca^{++} orbitals, $\Gamma_{15}(p^+)$, to high conduction bands. The loss at 27 eV is attributed to the core exciton transition $\Gamma_{15}(p^+) \rightarrow \Gamma_1$. The structure at 11 eV and 15 eV corresponds to resonant excitons associated with the allowed $\Gamma_{15} \rightarrow \Gamma_1$ and $X_5' \rightarrow X_3$ transitions, respectively.

The origins of the loss peaks at 3 and 7 eV are not as easily assigned. Visual examination of the damaged surface indicated that the electron beam had produced color centers (F-center), which are electron-containing fluorine ion vacancies. Both theoretical calculations[33] as well as optical absorption measurements[34] show that the optical transition energy of an F-center in calcium fluoride is 3.3 eV. This transition energy agrees with the observed low energy loss peak at 3 eV. Furthermore, the behavior of the 3 eV loss peak with increasing exposure of the calcium fluoride surface to high current density

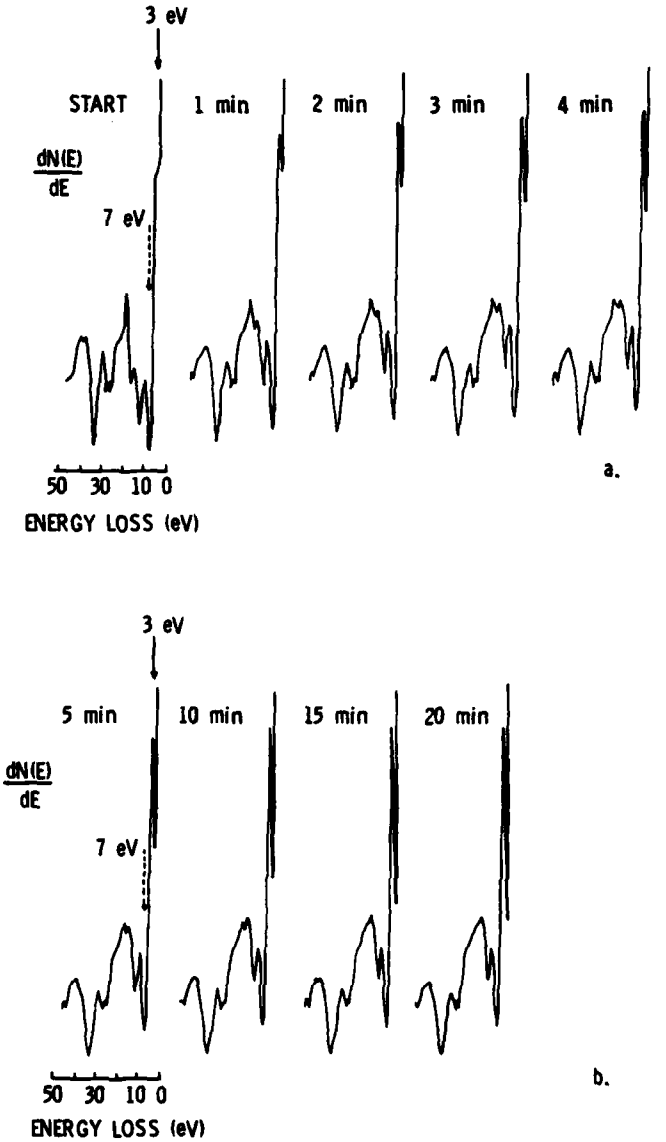

Figure 11. Energy-loss spectra of an air cleaved calcium fluoride surface excited with a 150 eV electron beam with increasing time of irradiation. (a) Initial sequence of ELS spectra, (b) final time sequence showing the increase in the 3 eV loss peak.

TABLE I. VALUES OF THE ENERGY LOSS PEAK OBSERVED FOR CALCIUM FLUORIDE

Characteristic Losses (eV): Present Work	Electron Transmission [a]	Optical Reflection [b]	Energy Losses Designation
3			F-centers[c]/Ep_s (Ca)[d]
7			Ep_b (Ca)[d]
11	11.8	11.18	$\Gamma_{15}(p^-)\rightarrow\Gamma_1$ exciton
15	15.8	15.4	$X_5'(p^-)\rightarrow X_3$ exciton
27	27.9	27.7	$\Gamma_{15}(p^+)\rightarrow\Gamma_1$ core exciton
33	33.6	32.8-34.5	$\Gamma_{15}(p^+)\rightarrow\Gamma_{25}'$, Γ_{12}

[a] Frandon et. al. Reference 30.

[b] Rubloff. Reference 32.

[c] Cavanett et. al. Reference 34.

[d] Robins et. al. Reference 35.

electron beam impact is typical of that expected for the increase in concentration of F-centers as time progresses. In addition, the gradual obliteration of the 15 eV loss peak concurrent with the increase in the 3 eV peak is consistent with the formation of fluorine vacancies, since the excitonic transition at 15 eV originates from the valence band composed of p F^- orbitals. However, color center formation does not explain the origin and behavior of the loss peak at 7 eV.

An alternative explanation, consistent with the observed ELS data, is that in addition to the formation of fluorine vacancies, the electron beam also causes the formation of calcium atoms in a metal-like state. Electron loss data have been reported for calcium metal by Robins and Best.[35] They noted loss peaks at 3.4, 8.8, 12.5, 27.4, 36.9, and 45.6 eV. The peaks at 27.4 and 45.6 eV were assigned to electronic transitions involving 3p and 3s metal electrons which have been promoted to states above the Fermi level. The highest intensity loss peaks observed by Robins and Best at 3.4 and 8.8 eV were assigned to surface and bulk plasmon excitations, respectively. The 12.5 eV loss was attributed to the combination of the surface and bulk plasmon loss.

The ELS data of Robins and Best for calcium metal indicates that the 3 and 7 eV loss peaks observed for electron decomposed calcium fluoride could result from surface and bulk plasmon excitations of calcium in a metallic-like state formed following the electron induced desorption of fluorine from the surface. In addition, the fact that the loss peak at 11 eV, which for calcium fluoride originates also from the p F^- valence band, does not decrease with electron bombardment, but remains constant and perhaps increases slightly, indicates that color center formation is not the only possible chemical change occurring at the surface during electron impact.

3. X-RAY PHOTOELECTRON MEASUREMENTS

In this section results on electron beam decomposition of cleaved calcium fluoride using a combination of XPS and XAES are presented. The study involved XPS and XAES measurements on the surface chemistry before electron bombardment and following electron bombardment by a 5 keV electron beam with a current density of about 0.2 mA/cm^2. After two hours of electron bombardment at this current density, the fluorine XPS and XAES integrated intensities were reduced by about 64 percent of their original intensities as shown in Figures 12 (a) and (b), respectively.

The change in the chemical state of the calcium ions before and after electron bombardment is shown in Figures 13 and 14. Figure 13 presents the XAES spectrum for the calcium $L_{2,3}MM$ Auger electron lines. A comparison of the two spectra shows that the electron beam damage resulted in a shift in the Auger lines by about 6 eV. In addition, it is seen that the intensities of the two predominant Auger transitions before and after electron irradiation are interchanged. However, the most pronounced effect of the electron impact is reflected in the calcium 2p photoemission spectra. As shown in Figure 14, the calcium 2p photoemission lines split into a second set of 2p photoemission lines at 2.4 eV lower in binding energy.

Along with the splitting of the calcium 2p photoemission line was an increase in the oxygen 1s photoemission peak as shown in Figure 15. The oxygen 1s photoelectron peak which is shifted to a higher binding energy following electron irradiation, is characteristic of adsorbed oxygen rather than a native oxide.[36,37] Throughout this study, the observed carbon 1s photoelectron signal indicated that carbon was present at a level of less than 1 atomic percent on the calcium fluoride surface.

We attribute the chemically shifted calcium 2p photoelectron peaks to lower binding energies to calcium ions in and near the

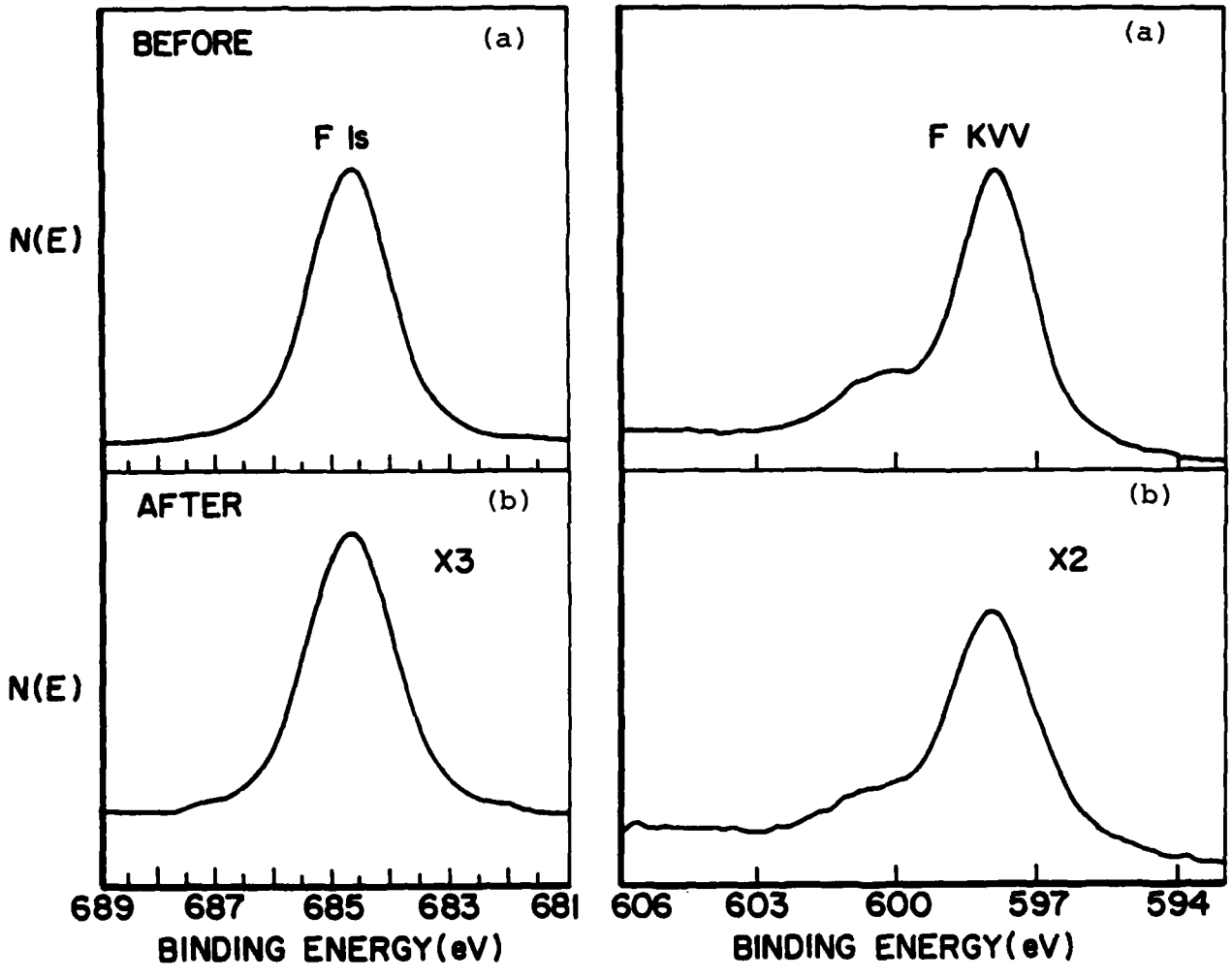

Figure 12. The fluorine signal of a cleaved calcium fluoride surface before and after two hours of electron bombardment with a 5 keV electron beam with a current density of 0.2 mA/cm^2. (a) the XPS spectrum of the fluorine 1s photoemission line; (b) the XAES spectrum of the fluorine KVV Auger transition.

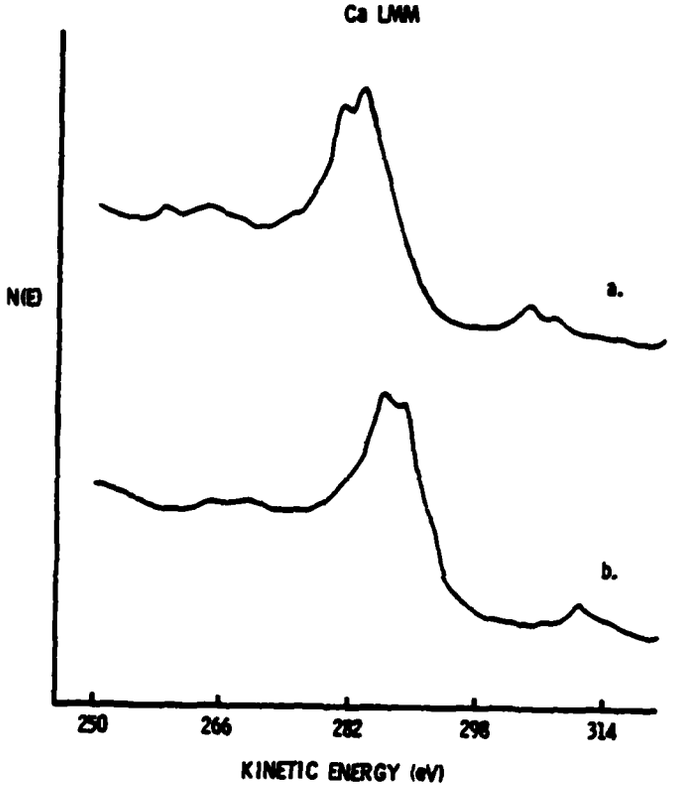

Figure 13. X-ray stimulated AES spectrum of a cleaved calcium fluoride surface showing the calcium LMM Auger transition: (a) before electron beam bombardment; (b) after two hours of electron bombardment with a 5 keV electron beam with a current density of 0.2 mA/cm^2.

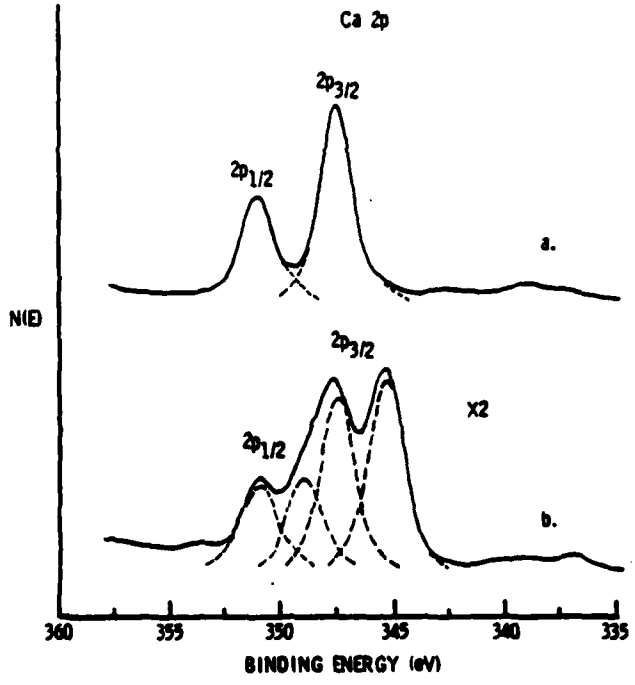

Figure 14. XPS spectrum of a cleaved calcium fluoride surface showing the calcium 2p photoemission lines: (a) before electron beam bombardment; (b) after two hours of electron bombardment with a 5 keV electron beam at 0.2 mA/cm^2.

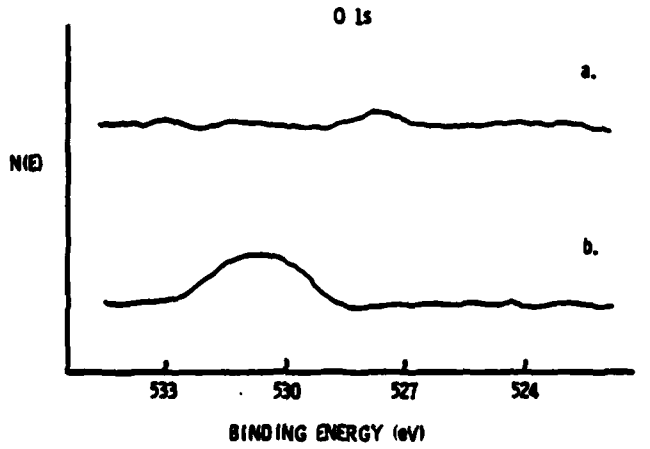

Figure 15. XPS spectrum of a cleaved calcium fluoride surface showing the oxygen 1s photoemission line: (a) before electron beam bombardment; (b) after two hours of electron bombardment with a 5 keV electron beam at 0.2 mA/cm^2.

surface which have undergone a reduction in coordination number because of the desorption of fluorine by the stimulus of the electron beam. Since the oxygen 1s photoelectron peak was observed to increase in intensity after electron irradiation, part of the shift in the calcium 2p photoemission lines may be associated with the reaction of oxygen atoms in the residual gas with the fluorine vacancies generated by the electron beam. However, when the calcium 2p photoelectron binding energy is referred to the fluorine 1s peak position (684.7 eV as measured by Wagner et. al.[38] for calcium fluoride), the binding energy for the shifted calcium $2p_{3/2}$ photoemission peak is determined to be 345.2 eV. This value is in good agreement with the calcium $2p_{3/2}$ binding energy measured by Van Doveren and Verhoeven[39] for calcium metal (345.7 eV). Furthermore, the calcium $2p_{3/2}$ photoelectron peak assigned to calcium fluoride has a binding energy which is within 0.2 eV of that reported by Wagner[40] (347.7 eV).

SECTION V

ISS ANALYSIS - CRYSTAL ORIENTATION EFFECTS

Ion scattering spectroscopic analysis was performed on as-prepared, cut and polished (100) and (110) surfaces, and on cleaved (111) calcium fluoride surfaces. The effect of primary beam energy using $^3He^+$ ions, on the ISS spectra for a cleaved (111) calcium fluoride surface is shown in Figure 16. It can be seen that as the primary ion beam energy is increased, the background correspondingly increases, resulting mainly from multilayer scattering.[41] The ISS spectra for the (100) and (110) surfaces showed similar signal to background variations with primary beam energy.

When analyzing a multicomponent surface with ISS, preferential sputtering of one constituent over another may occur. In Figure 17, the relative peak heights for calcium and fluorine are shown as a function of bombardment time for a 1.0 keV $^3He^+$ ion beam. It is seen that neither the calcium nor fluorine scatter peaks change substantially with time, suggesting that uniform removal of the surface atoms is taking place. The sputtering rate for a 1.0 keV $^3He^+$ beam with 1 $\mu A/mm^2$ current density is less than 1Å/minute.

The effect of ion beam energy on the backscattered ion intensities for calcium fluoride surfaces was obtained by measuring the relative peak heights of calcium and fluorine at beam energy intervals of 0.5 keV. As the specimen was sputtered, spectra were taken at intervals of about 1 minute. Initial scans often showed changing peak heights. The "steady state" was taken when the calcium peak heights remained constant for at least 5 scans.

To compare the ISS data for three surface orientations, the calcium to fluorine ratios for each orientation were determined. Figure 18 shows the dependence of these ratios as a function of primary ion beam energy. These ratios were adjusted for the

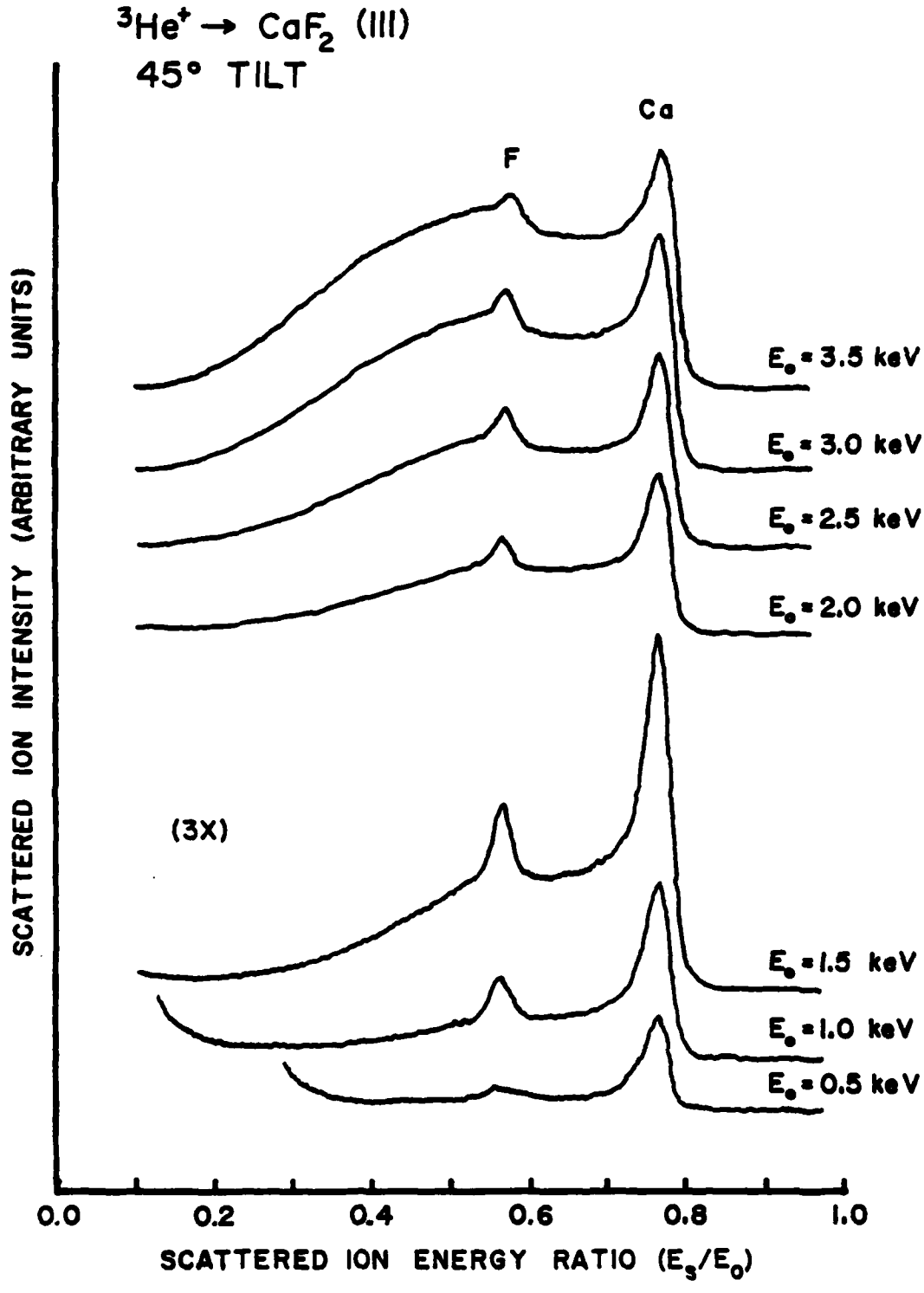

Figure 16. Comparison of ISS spectra at various initial $^3He^+$ ion beam energies, E_o, for a calcium fluoride (111) face which was tilted 45 degrees with respect to the incident ion beam.

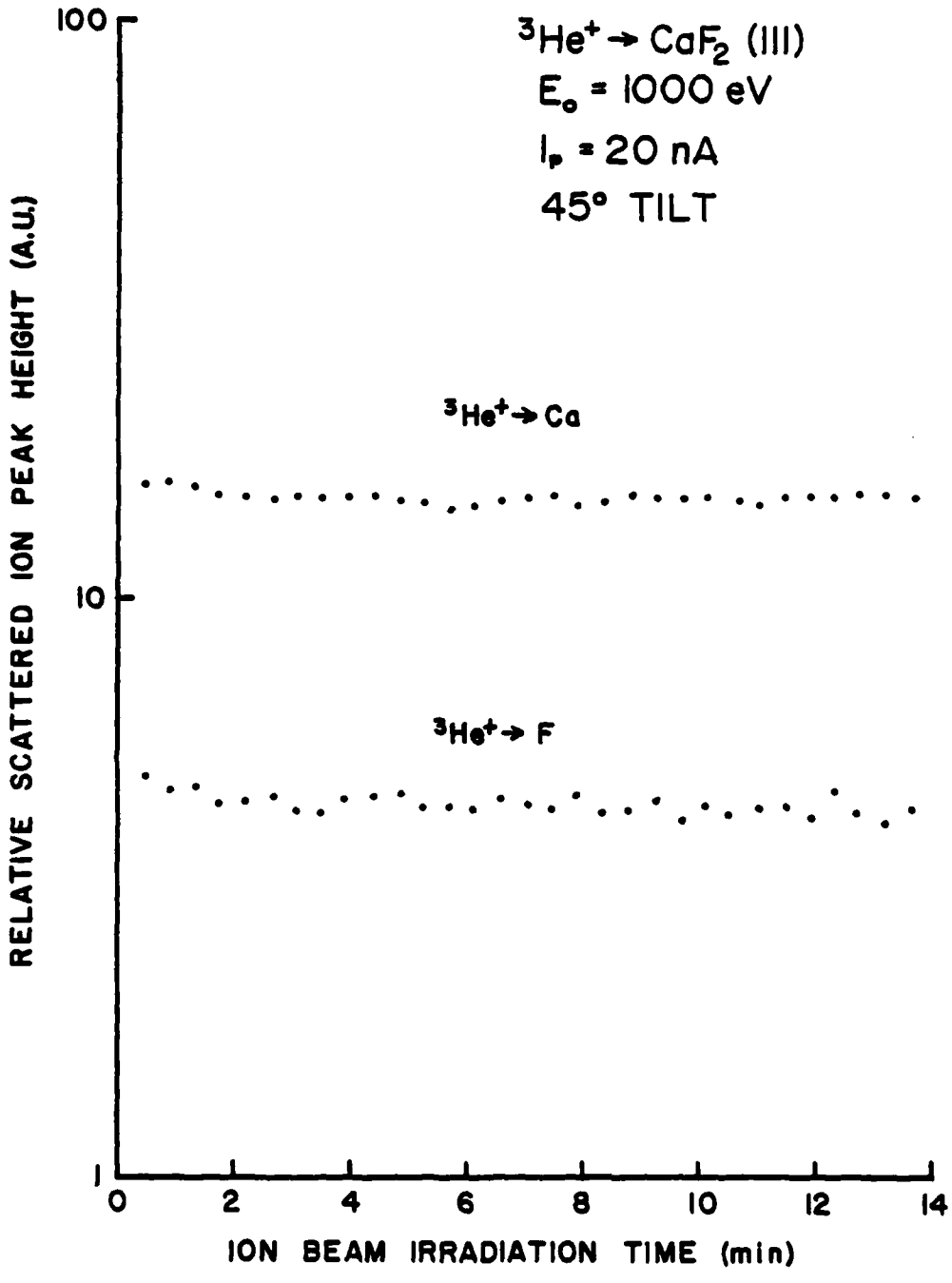

Figure 17. The relative amplitude of the scattered ion peak of calcium and fluorine as a function of exposure time to ion bombardment for a 1.0 keV $^3He^+$ ion beam.

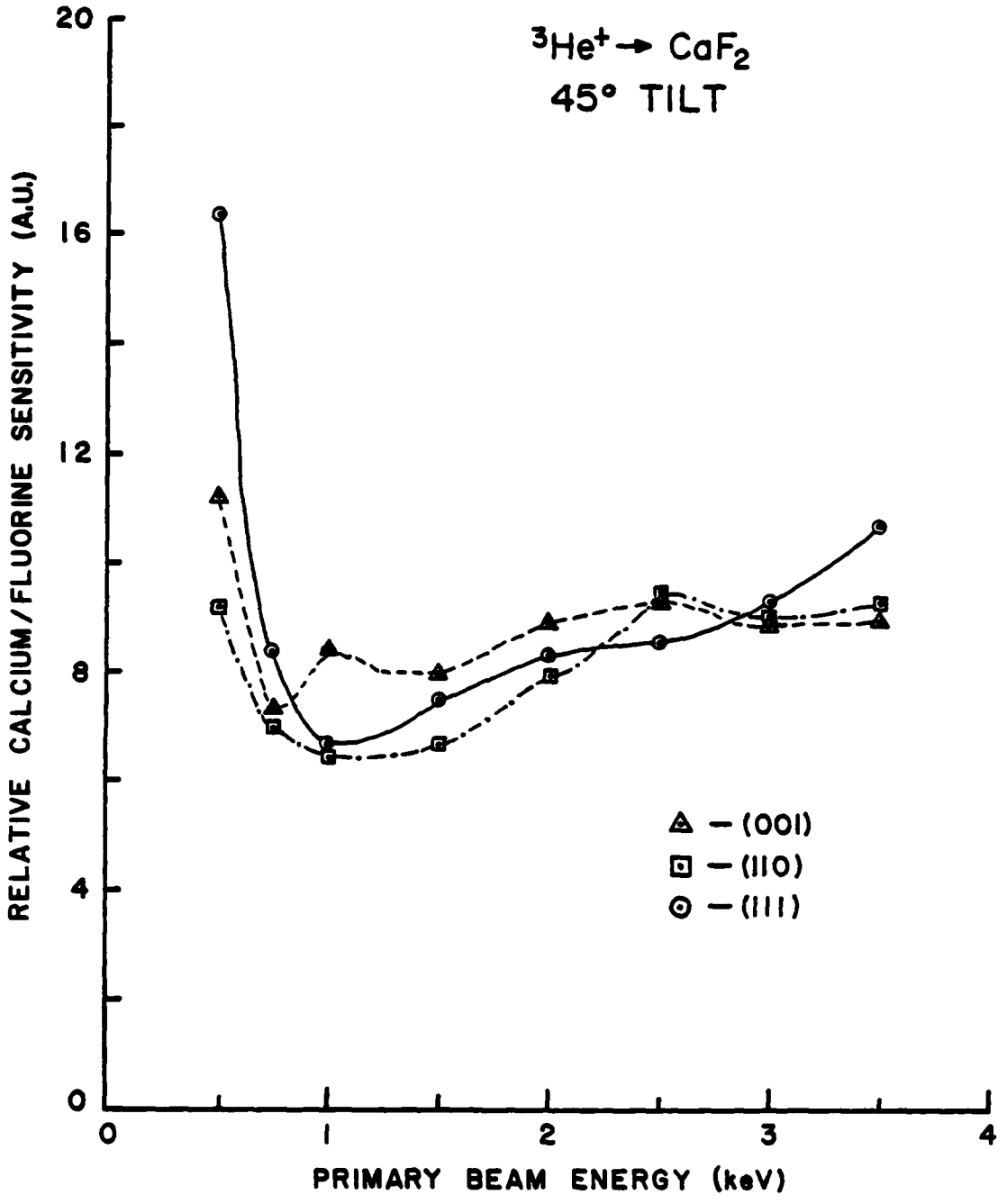

Figure 18. Variation of the calcium to fluorine sensitivity with probe energy for $^3He^+$ ISS of CaF_2, cut and polished, (001) and (110), and cleaved (111) faces.

atom density of calcium fluoride. It can be seen that for each orientation, the results showed enhanced sensitivity to scattering from fluorine at a primary ion energy of approximately 1 kilovolt. This is attributed to a combination of ion neutralization and atom shielding effects.[42]

It is also interesting to note that the ratios for each of the surfaces are not significantly different above a primary beam energy of 1 keV. This is expected for two reasons. First, the increase in the background due to multilayer scattering masks any subtle differences in stoichiometry between the surfaces. Secondly, based on a rigid sphere model for each surface orientation, the smallest void within a plane is still about 1.5 times larger than the radius of the $^{3}He^{+}$ ion ($r_{He^{+}} \approx 0.4\text{Å}$). Consequently, the $^{3}He^{+}$ ions can scatter from atoms in the second and possibly even the third layer below the surface. As a result, little difference in the calcium to fluorine ratio is observed between the (100), (110) and (111) planes.

SECTION VI
WATER ADSORPTION ON CLEAN CALCIUM FLUORIDE SURFACES

In this section we report on ion scattering spectroscopic measurements of the adsorption of water on clean calcium fluoride surfaces.

Calcium fluoride specimens were prepared in air and placed in the ISS analysis chamber. After baking of the spectrometer, the specimens were argon sputter etched for 10 minutes using a 1 keV ion beam with a current density of 12 nA/cm^2. These specimens were exposed to various amounts of water vapor and adsorption isobars were obtained by the temperature variation method. Exposures were accomplished experimentally by dynamically flowing water vapor at constant pressure through the ISS analysis chamber with the specimen maintained at a preselected temperature and, after a designated period of time, ISS spectra recorded. The temperature of the specimen was then changed and a new set of ISS spectra taken as a function of exposure time. This procedure was repeated for the range of temperatures from 180-300 K. Water pressures in the range of 10^{-6}-10^{-5} Pa were employed in these experiments. The pressure was measured with a nude Bayard-Alpert ion gauge, and the water vapor purity monitored with a quadrupole mass spectrometer. Ionization gauge readings were corrected for water using a sensitivity factor of 1.1.[43]

The ISS results from the initial adsorption experiments indicated that the 1000 eV $^3He^+$ ion beam caused hydrolysis of the calcium fluoride surface during exposure to water. This ion beam-induced damage was found to be dependent on the current density of the probe ion beam. When the ISS analysis of a water exposed calcium fluoride surface was performed with an ion beam having a current density of 180 nA/cm^2 or greater, the oxygen signal was observed to decrease about 40 percent wthin 24 hours after exposure while subject to pressure of less than 2×10^{-8} Pa. However, no further reduction in the oxygen signal could be

achieved either by heating the specimen to 385 K or prolonged argon sputter etching. The observed ISS oxygen signal indicated that oxygen (or oxide) was present at a level of about 11 atom percent on the calcium fluoride surface. On the other hand, it was found that by rastering the ion beam during the analysis to achieve a current density of less than 80 nA/cm^2, an adsorbed water layer could be readily removed by exposure to UHV conditions at room temperature, so that no oxygen signal was observed within the detection limits of ISS (limit of detectability being 1 percent of a monolayer).[44] Consequently, all of the succeeding ISS spectra were measured using a rastered $^3He^+$ ion beam with a primary energy of 1000 eV and a current density of 80 nA/cm^2.

Exposure of an argon sputter cleaned calcium fluoride surface to water vapor at 300 K resulted in the sequence of ISS spectra shown in Figure 19. The measurements were taken under conditions of a dynamic equilibrium, so that water molecules which are sputtered by the He ion beam are replaced by water molecules from the gas phase. The intensity of the ISS oxygen signal reached a maximum after water exposures >10 L* and is independent of water pressure in the range from 10^{-6}-10^{-5} Pa. Overnight exposure to UHV conditions within the ISS specimen chamber at room temperature readily removed the water adsorbed on the calcium fluoride surface and did not lead to surface hydrolysis as shown in Figure 19(e).

As can be seen in Figure 19, a broad, low intensity peak is centered around a scattered ion energy ratio, E/E_o, of 0.4. The intensity of this peak was found to increase almost two-fold by either increasing the water pressure in the chamber or lowering the surface temperature of the specimen. The origin of this peak is not known. Numerous authors have noted in passing a similar low energy "sputter" peak,[18,41] but as yet no satisfactory

---

*1 L = 1 Langmuir = 10^{-6} Torr sec = 1.3×10^{-4} Pa sec = 4.9×10^{14} molecules cm^{-2} sec^{-1} (H_2O at 300 K).

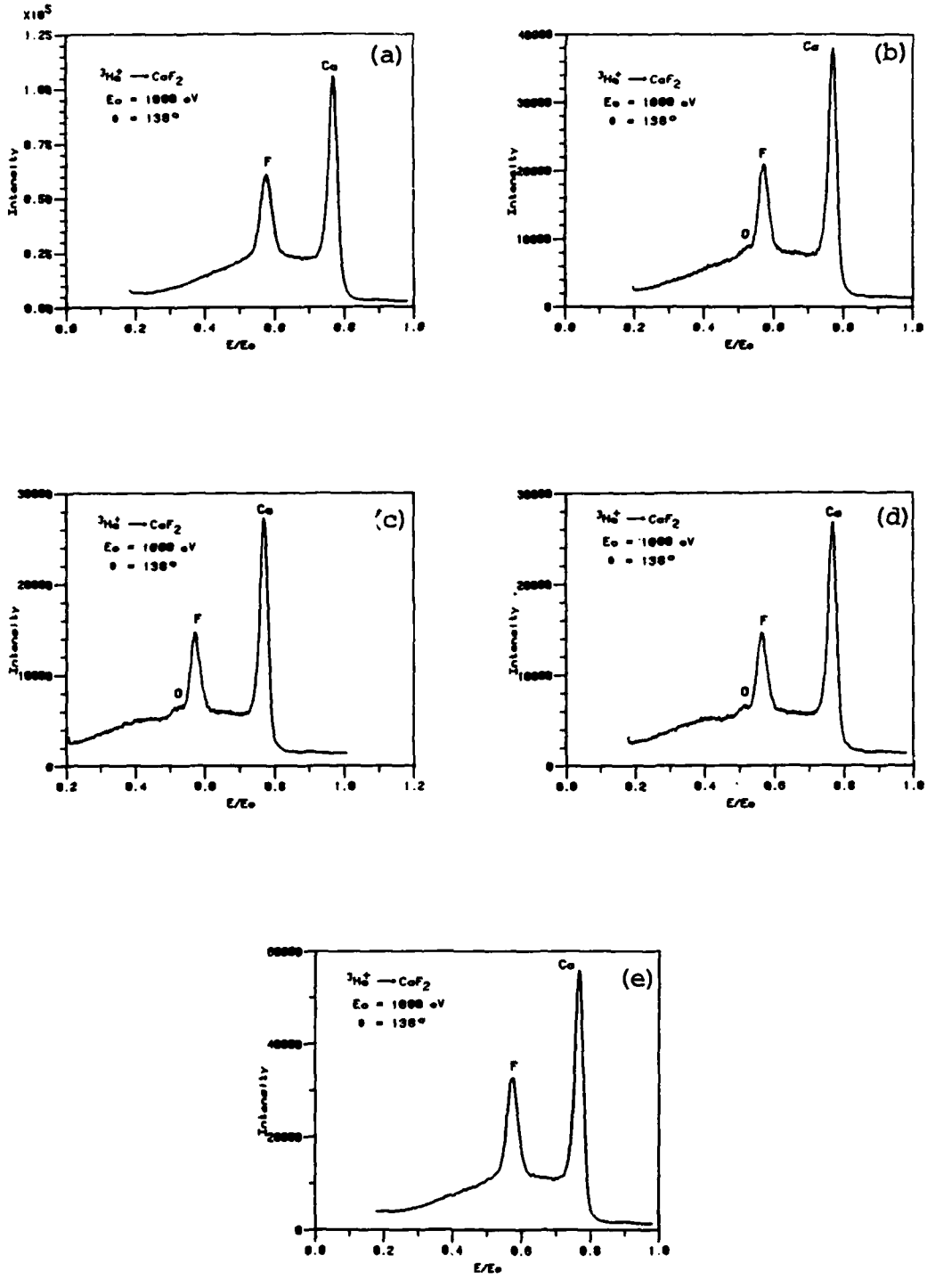

Figure 19. ISS spectrum of a calcium fluoride surface: (a) after argon sputtering; after 20 minute exposure to water (b) at P_{H_2O} = 1.3 x 10^{-6} Pa; (c) at P_{H_2O} = 6.7 x 10^{-6} Pa; (d) at P_{H_2O} = 1.3 x 10^{-5} Pa; and (e) after overnight exposure to UHV conditions. The surface temperature of the specimen was at 300 K.

explanation has been put forth. Helium ion scattering from carbon does result in a backscattered ion peak at an energy ratio of 0.41. G. E. Thomas et. al.[45] have shown that ISS is about 45 times more sensitive to oxygen than carbon for He^+ ions at probe energy of 1500 eV. As a result of this low sensitivity it is unlikely that carbon is the source of this forepeak, particularly when the partial pressure of the carbon containing gases (e.g., CH_4, CO, CO_2) present in the residual gas is less than 12 percent of the water pressure used in these studies. G. E. Thomas et. al. also observed a similar forepeak in the ISS spectra of polymers. They suggested that this is due to H^+ ions sputtered by relatively hard collisions with He^+ backscattered from deeper layers and/or is due to He^+ backscattered after multiple collisions and possibly reionized at the surface.

The extent to which the water coverage on the calcium fluoride surface is affected by surface temperature is illustrated in Figure 20. In this experiment an air cleaved calcium fluoride surface was cleaned by sputter etching with argon at 1000 eV for 10 minutes. The specimen was then exposed to water at a fixed pressure of 1.3×10^{-6} Pa for approximately one hour at 300 K, during which time the surface was periodically examined with helium ISS. The surface temperature was then lowered to a different temperature and a new set of ISS spectra recorded. As seen in Figure 20, the increase in the oxygen signal is monotonic and reaches a maximum below a surface temperature of 185 K. In contrast to this, both the calcium and fluorine signals fall-off rapidly below 220 K, with the calcium signal diminishing to background level at a surface temperature of 180 K. Since both the calcium and fluorine ISS signals decreased concurrently with decreasing temperature (increasing surface coverage of water) ion neutralization effects are not considered to be the dominant factor in the reduction of the calcium signal to background level at 180 K. Rather, the attenuation of the calcium signal is attributed to geometrical shadowing of calcium by the adsorbed

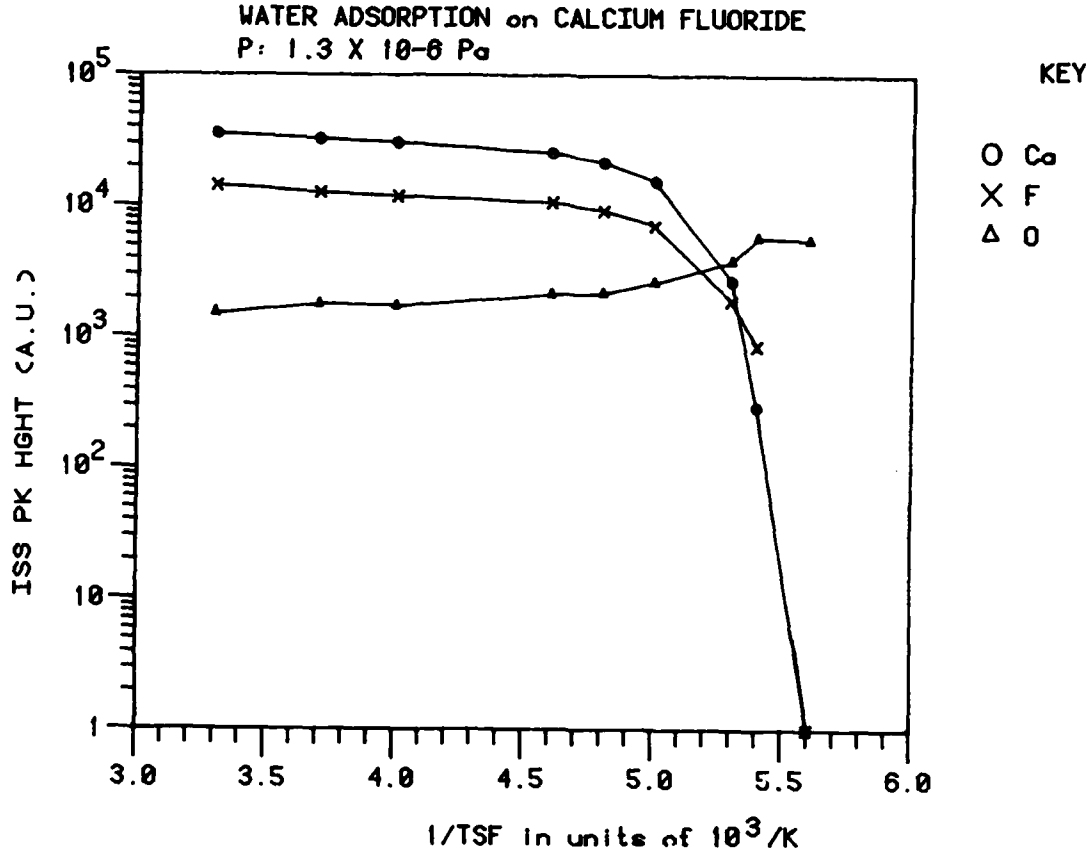

Figure 20. Temperature dependence of the $^3He^+$ ion scattering signals for water adsorption on argon sputter cleaned calcium fluoride. Maximum coverage is about one monolayer.

water molecules. As for the fluorine signal, below a temperature of 190 K the helium scattering peak from fluorine becomes unresolved underneath the high energy tail of the oxygen ISS peak. The ISS spectra taken below a temperature of 200 K illustrates these changes (see Figure 21).

Unlike the room-temperature adsorption studies, pumping on the specimen did not significantly change the relative intensities of the calcium, fluorine, and oxygen ISS peak as shown in Figure 23. After the specimen reached room temperature the ISS spectrum in Figure 22(a) was obtained while maintaining the water at 1.3×10^{-6} Pa. Spectrum (b) was obtained after evacuation of the ISS spectrometer for 60 hours at room temperature. The base pressure of the specimen chamber was 3×10^{-8} Pa. Heating the specimen to 340 K for 30 minutes did result in a small reduction in the intensity of the oxygen peak, Figure 22(c). However, after argon sputter etching the specimen for 20 minutes at 340 K, the calcium and fluorine ISS peaks increased almost four-fold in intensity while the oxygen peak was reduced to background level as shown in Figure 22(d).

From the ion scattering results shown in Figure 20 it is possible to suggest a model for the adsorption of water on calcium fluoride. Because of the classical nature of the ion scattering process, adsorbed species can cause geometrical shadowing to occur so that the incident ions cannot collide directly with an atom A which lies behind another atom B. As previously noted, at a given surface temperature and water pressure only the calcium signal goes to background level indicating that the adsorbed water molecules are shadowing the calcium ions. This can occur if the water molecule hydrogen-bonds between two fluorine ions in the surface. In fact, assuming an fluorine-oxygen length of 2.50 Å, which is the sum of the fluorine-hydrogen bond distance (1.55 Å) in hydrogen fluoride vapor[46] and the oxygen-hydrogen bond distance (0.957 Å) in ice[47], the the resulting value of 100.8° for the water bond angle (using a

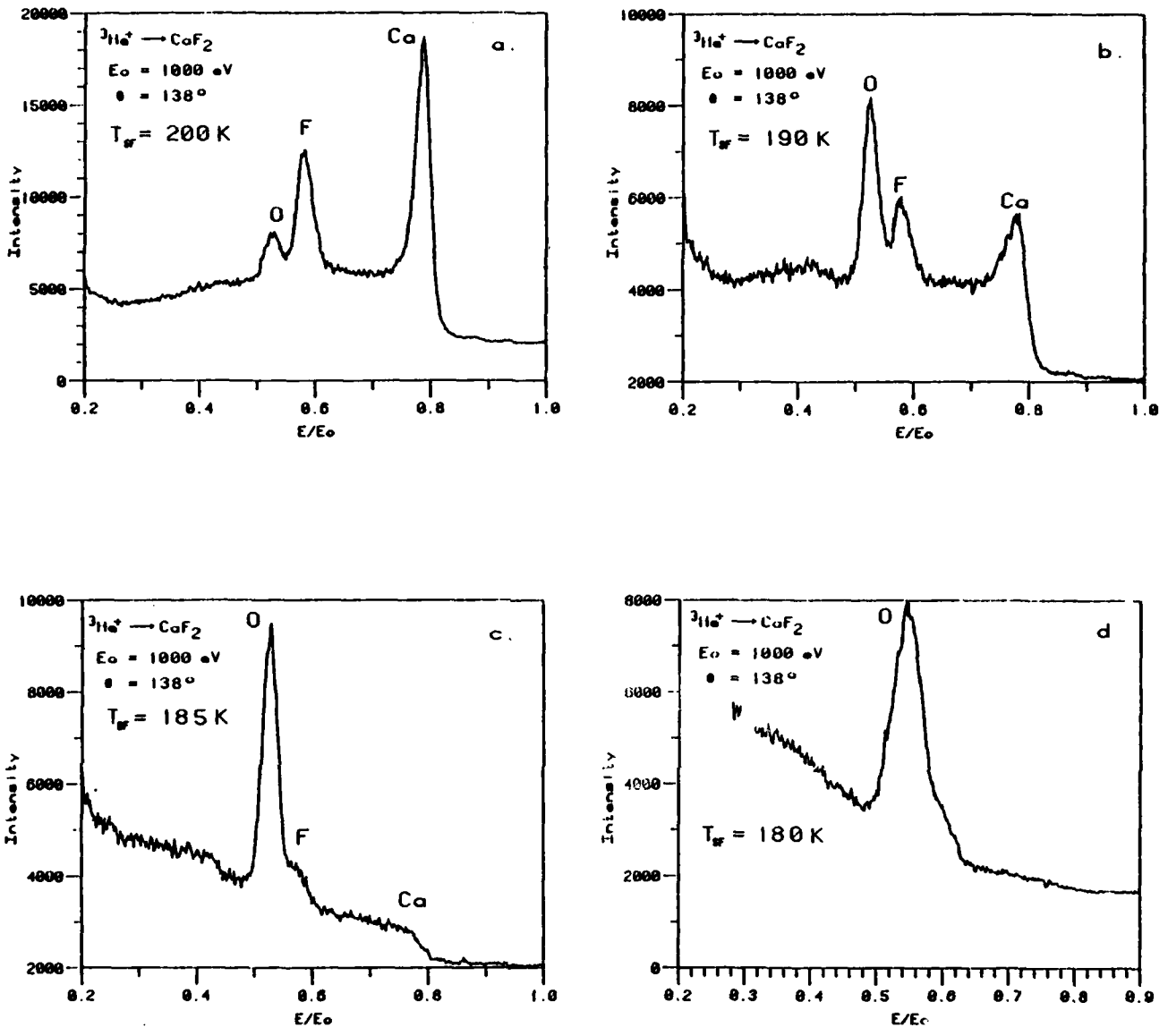

Figure 21. ISS spectrum of a cleaned calcium fluoride specimen exposed to water at P_{H_2O} = 1.3 x 10^{-6} Pa with a surface temperature of (a) 200 K, (b) 190 K, (c) 185 K and (d) 180 K.

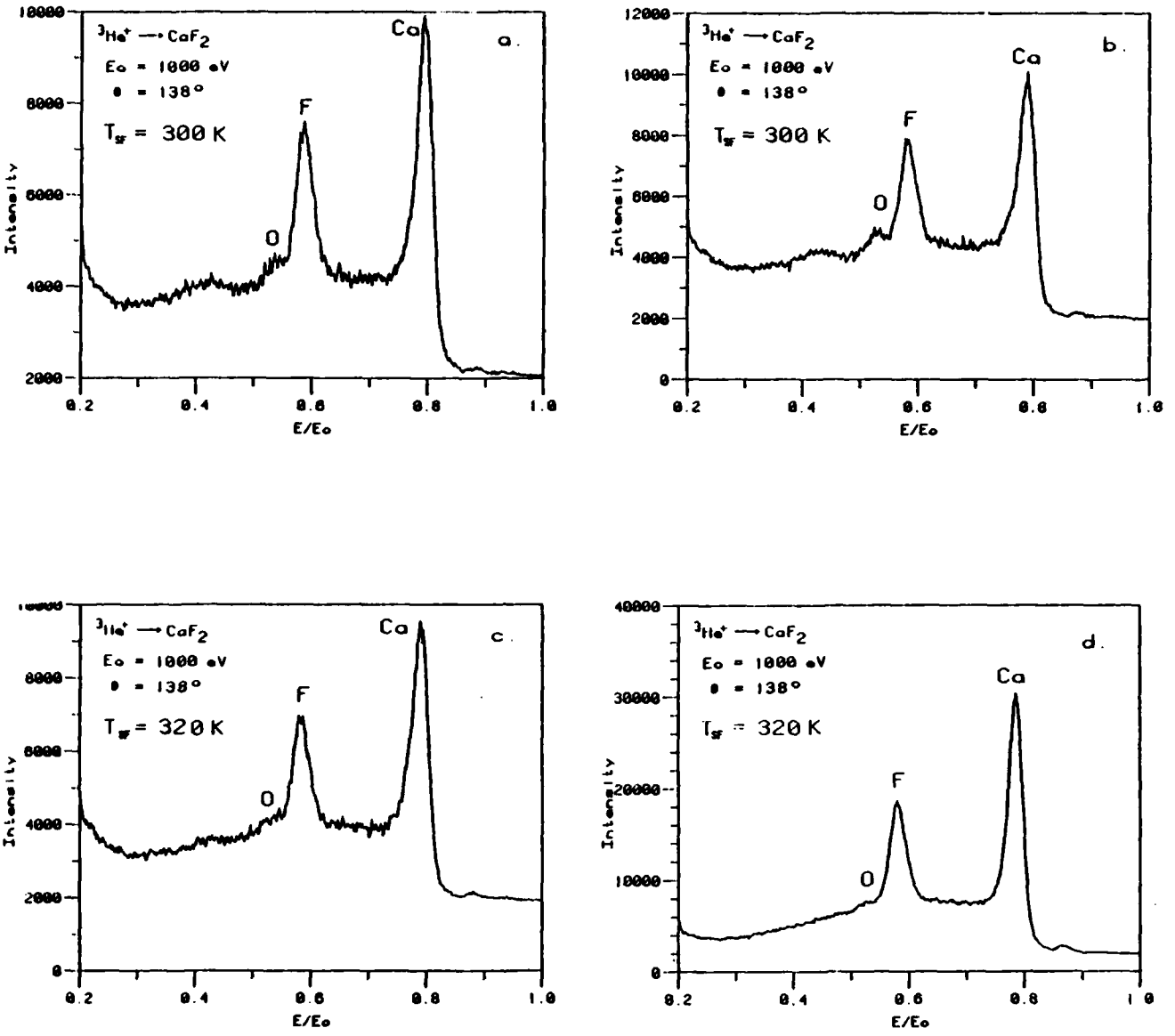

Figure 22. Helium ISS spectrum of a cleaned calcium fluoride surface and sputtered with $^3He^+$ at 1 keV. (a) heated from 180 K to 300 K during exposure to water at P_{H_2O} = 1.3 x 10^{-6} Pa; (b) exposed to UHV conditions for about 60 hours; (c) heated to 340 K for 30 minutes; and (d) after 20 minutes of sputter etching with argon at 1 keV and a current density of 12 nA/cm^2.

fluorine distance of 3.86 Å for the (111) surface) is not greatly distorted from its normal value of 104.5°. Thus, a water molecule with its polar axis perpendicular to the surface and with the hydrogen atoms adjacent to the surface could quite easily bridge two fluorine ions, and a close packed arrangement of water molecules oriented in this manner could be built up as schematically shown in Figure 23.

For the purpose of this work, a monolayer capacity is defined as the amount of exposure needed to cover the whole surface with an adsorbed layer of one molecular thickness. Experimentally the water exposure at which the calcium ISS signal disappears has been established as monolayer coverage. Since the ion scattering signal and surface coverage are proportional[48], it is possible to normalize the oxygen signal to the fraction of a monolayer of water adsorbed on the calcium fluoride surface. As a result, the oxygen signal observed at 300 K for the as-cleaned surface (see Figure 20) represents a water coverage of approximately one-fourth of a monolayer. For surface coverage greater than a monolayer the oxygen ISS signal saturates and does not increase linearly with increasing coverage as seen in Figure 20.

With the assumption that a monolayer coverage occurs when the calcium ISS signal diminishes to background level, the isosteric heat of adsorption, Q_{st}, is determined to be 10.8 ±0.6 kcal/mole using the Clausius-Clapeyron relationship:

$$\left[\frac{d \ \ell n \ P}{d \ (1/T)}\right]_{\Theta = \text{const}} = - \frac{Q_{st}}{R}$$

where R is the universal gas constant (1.987 cal/K mole), P is the partial pressure of water and T the surface temperature at a given surface coverage, Θ. The similarity of this value to the heat of liquefaction for water (10.5 kcal/mole) seems to suggest a single hydrogen-bonding interaction per water molecule with the calcium fluoride surface. If a double bond were formed and the adsorbed water molecules were oriented as in Figure 23, a value

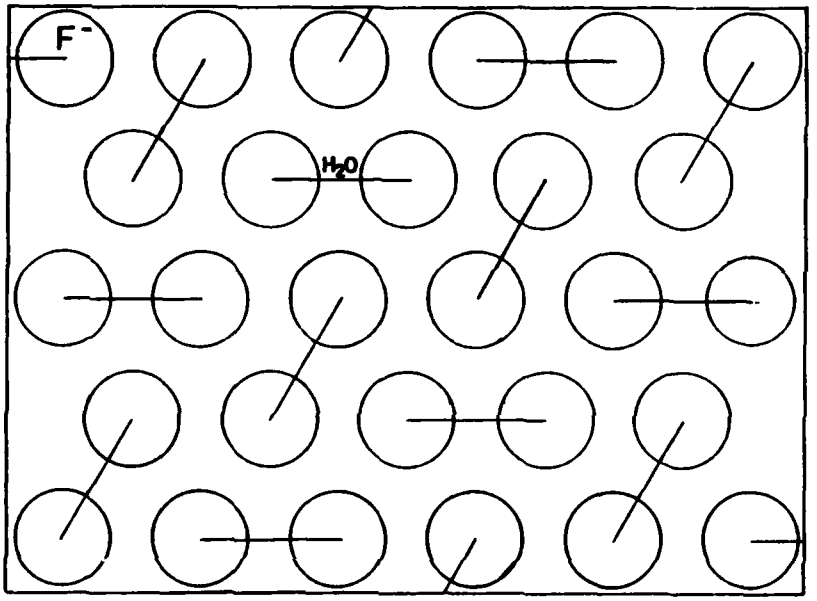

Figure 23. A possible bridging of fluorine ions by water molecules in the (111) plane of calcium fluoride.

of Q_{st} in excess of 12 kcal/mole would be expected. This theoretical value of 12 kcal/mole was calculated as twice the average of the experimental values for gaseous F-H··· F (7 kcal/mole) and gaseous O-H··· O (5 kcal/mole), that is, 6 kcal/mole per hydrogen bond.[49] The magnitude of Q_{st} is, however, consistent with the heat of adsorption for water on calcium fluoride powders determined by Hall, Lovell, and Finkelstein.[11] It is interesting to note that their results showed that the isosteric heat of adsorption is in excess of 12 kcal/mole for water coverages less than 1/2 a monolayer, but decreases to approximately that of the heat of liquefaction for water at surface coverages equal to and greater than a monolayer. The uncertainty in the heat of adsorption reported in this work is estimated to be ±0.61 kcal/mole based on the fluctuation in surface temperature of ±0.5 K.

SECTION VII
CONCLUSIONS

The results obtained during this research program are substantial and broad in scope. An argon sputter etching technique can be used to prepare uncontaminated calcium fluoride surfaces. Both AES and ISS measurements before, during, and after the argon sputter etching of an air cleaved calcium fluoride surface showed a reduction in surface carbon contamination accompanied by an appropriate increase in the calcium signal as a function of sputter time. Furthermore, the fluorine AES/ISS peaks showed little variation during the sputtering process indicating that selective sputtering of the fluorine had not occurred.

It was observed in the early stages of the program that calcium fluoride decomposed under electron beam impact when using typical AES electron beam parameters (5 keV, 5 μA). Using the combined techniques of AES, ELS, and XPS, this decomposition was identified as the electron-induced desorption of fluorine and a simultaneous accumulation of F-centers and metallic-like calcium on the surface. The electron damaged calcium fluoride surfaces were particularly sensitive to oxygen and oxidized readily with the residual component gases in the different spectrometers. The rate of fluorine desorption was found to depend upon the time of exposure and the current density of the incident electron beam. Threshold measurements for the onset of fluorine desorption showed that AES analysis could be made without producing significant electron-beam damage by rastering a 2.5 keV electron beam using a current density of 0.16 mA/cm^2 or less.

Initial ISS studies involved the measurement of the $^3He^+$ scattering peak intensities from calcium and fluorine as a function of primary beam energy (0.5-3.5 keV) for cleaved (111), cut and polished (100) and (110) calcium fluoride specimens. Results from these measurements indicated an enhanced sensitivity to scattering from fluorine at a $^3He^+$ ion energy of about 1 keV.

Furthermore, the calcium to fluorine ratios for each of the surfaces were not found to be significantly different at beam energies greater than 0.75 keV. This is attributed to the fact that the He^+ ionic radius is small enough to allow the ion to penetrate the second or third atomic layer without incurring a substantial energy loss.

The adsorption of water by argon sputter cleaned calcium fluoride surfaces was investigated using ISS. A temperature variation method was employed to determine adsorption isobars. Room-temperature exposure of a clean calcium fluoride surface to water in the pressure range of 10^{-6}-10^{-5} Pa resulted in an almost instantaneous saturated surface coverage of about a 1/4 monolayer. Removal of this adsorbed water layer was readily achieved by prolonged exposure to UHV conditions at room temperature. At a surface temperature of T_{SF} = 180 K and a water partial pressure of 1.3×10^{-6} Pa, an immediate coverage of one monolayer resulted. It was further observed that water coverages produced on specimens below room temperature would not desorb solely by prolonged exposure to UHV conditions, but required a combination of argon sputter etching and heating of the specimen to 320 K before the water was removed. This suggests perhaps two different states of adsorption which are temperature dependent. ISS measurements confirmed that surface hydrolysis did not occur because the oxygen ISS peak could be reduced to background level by heating and ion sputtering the specimen.

The heat of adsorption of water on argon sputter cleaned calcium fluoride was determined from the ISS results to be 10.8 ±0.6 kcal/mole. The magnitude of this quantity is consistent with single hydrogen bonding between the adsorbed water molecule and the calcium fluoride surface. However, the rapid fall-off of the calcium ISS peak to a background level with increasing water coverage (lower surface temperature) suggests that the water molecules are adsorbed in a bridge position between two fluorine atoms, resulting in a double hydrogen bond. Conclusions about

the exact adsorption site are not possible with the data reported here. Further studies on the azimuthal dependency of the back-scattered ion intensity from water and calcium fluoride would prove very helpful in elucidating the orientation of the adsorbed water molecule on the calcium fluoride surface.

REFERENCES

1. C. B. Willingham, Fusion Casting of Alkaline-Earth Fluorides for High-Power Laser Windows, Final Report, AFML-TR-78-188, DARPA, Contract No. F19628-76-C-0279, January 1979.

2. J. A. Harrington, et al, Fifth Conference on High-Power Infrared Laser Window Materials, C. R. Andrews and C. L. Strecker, eds., February 1976, page 872.

3. T. F. Deutsch, J. Phys. Chem. Solids 34, 2091 (1973).

4. F. A. Horrigan and T. F. Deutsch, Research in Optical Materials and Structures for High-Power Lasers, Final Technical Report, DARPA Contract No. DAAH-1-70-C-1251, Sept. 1971, p. 82.

5. A. L. McClellan and H. F. Harnsberger, J. Colloid Interface Sci. 23, 557. (1963).

6. J. H. de Boer and C. J. Dippel, Z. Phys. Chem. 21, 198 (1933).

7. J. H. de Boer and C. J. Dippel, Z. Phys. Chem. 21, 278 (1933).

8. J. H. de Boer and C. J. Dippel, Z. Phys. Chem. 25, 399 (1934).

9. C. B. Amphlett, Trans. Faraday Soc. 54, 1206 (1958).

10. P. G. Hall and F. C. Tompkins, Trans. Faraday Soc. 58, 1734 (1962).

11. P. G. Hall, V. M. Lovell and N. P. Finkelstein, Trans. Faraday Soc. 66, 1520 (1970).

12. P. B. Barraclough and P. G. Hall, Surface Sci. 46, 393 (1974).

13. P. B. Barraclough and P. G. Hall, J. Chem. Soc. Faraday Trans. I 71, 2266 (1975).

14. E. D. Palik, J. W. Gibson and R. T. Holm, Surface Sci. 84, 164 (1979).

15. C. B. Willingham, Fabrication Process Development of Alkaline Earth Fluorides for High-Power Laser Windows, Final Report AFWAL-TR-80-4200, USAF, Contract No. F33615-77-C-5127, Mar. 1981.

16. D. J. Ball, T. M. Buck, and D. MacNair, and G. H. Wheatley, Surface Sci. 30, 69 (1972).

17. R. G. Hart and G. Burleigh Cooper, Surface Sci. 82, L283 (1979).

18. H. H. Brongersma and P. Mul, Surface Sci. 35, 393 (1973).

19. E. Taglauer and W. Heiland, App. Phys. 9, 261 (1976).

20. W. Heiland and E. Taglauer, J. Vac. Sci. Technol. 9, 620 (1972).

21. W. Heiland, F. Iberl and E. Taglauer, Surface Sci. 53, 383 (1975).

22. E. Taglauer and W. Heiland, Appl. Phys. Lett. 24, 437 (1974).

23. E. Taglauer and W. Heiland, Surf. Sci. 47, 234 (1975).

24. G. A. Graves, et al, Exploratory Development on the Multidisciplinary Characterization of Infrared Transmitting Materials, Final Report, AFML-TR-79-4152, USAF, Contract No. F33615-77-C-500A, Oct. 1979.

25. C. G. Pantano and T. E. Madey, Appl. Surf. Sci. 7, 115 (1981).

26. J. T. Grant, R. G. Wolfe, and M. P. Hooker, J. Vac. Sci. Technol. 14, 232 (1977).

27. H. N. Hersch, Phys. Rev. 148, 928 (1966).

28. D. Pooley, Proc. Phys. Soc. (London) 87, 245 (1966).

29. M. L. Knotek and P. J. Feibelman, Surf. Sci. 90, 78 (1979).

30. J. Frandon, B. Lahaye, and F. Pradal, Phys. Stat. Sol. 53, 565 (1972).

31. J. P. Albert, C. Jouanin, and C. Gout, Phys. Rev. B 16, 4619 (1977).

32. G. W. Rubloff, Phys. Rev. B 5, 662 (1972).

33. H. S. Bennett, Phys. Rev. B 3, 2763 (1971).

34. B. C. Cavanett, W. Hayes, I. C. Hunter, and A. M. Stoneham, Proc. Roy. Soc. (London) A 309, 53 (1969).

35. J. L. Robins and P. E. Best, Proc. Phys. Soc. (London) 79, 110 (1962).

36. T. Robert, M. Bartel, and G. Offergeld, Surf. Sci. 33, 123 (1972).

37. J. C. Fuggle, L. M. Watson, D. J. Fabian, and S. Affrosman, Surf. Sci. 49, 61 (1975).

38. C. D. Wagner, L. H. Gale, and R. H. Raymond, Anal. Chem. 51, 466 (1979).

39. H. Van Doveren and J. A. TH. Verhoeven, J. Electron Spectrosc. Relat. Phenom. 21, 265 (1980).

40. C. D. Wagner, Discuss. Faraday Soc. 60, 291 (1975).

41. W. L. Baun, Appl. Surf. Sci. 1, 81 (1977).

42. R. C. McCune, Appl. Surf. Sci. 5, 275 (1980).

43. R. L. Summers, Empirical Observations on the Sensitivity of Hot Cathode Ionization Type Vacuum Gages, NASA Technical Note TND-5285, National Aeronautics and Space Administration, Washington, DC, June 1969.

44. A. W. Mullendore, G. C. Nelson, and P. H. Holloway, in Proceedings of the Advanced Techniques in Failure Analysis, IEEE Catalog No. 77CH1248-4REG6, Sept. 1977, page 236.

45. G. E. Thomas, G. C. J. van der Ligt, G. J. M. Lippits and G. M. M. van de Hei, Appl. Surf. Sci. 6, 204 (1980).

46. S. H. Bauer, J. Am. Chem. Soc. 61, 19 (1939).

47. A. F. Wells, Structural Inorganic Chemistry, 3rd ed., (Oxford University Press, London, 1962), p. 566.

48. W. Englert, W. Heiland, E. Taglauer and D. Menzel, Surf. Sci. 83, 243 (1979).

49. G. C. Pimental and A. L. McClellan, The Hydrogen Bond, (Freeman, San Francisco, 1960).

APPENDIX A

Electron-beam-induced decomposition of ion bombarded calcium fluoride surfaces

Charles L. Strecker
Air Force Wright Aeronautical Laboratories, Materials Laboratory, Wright-Patterson AFB, Ohio 45433

W. E. Moddeman [a] and J. T. Grant
Research Institute, University of Dayton, Dayton, Ohio 45469

(Received 20 April 1981; accepted for publication 15 July 1981)

The effects of electron beams on the composition of ion bombarded calcium fluoride surfaces have been studied with Auger electron spectroscopy (AES), electron loss spectroscopy (ELS), and x-ray photoelectron spectroscopy (XPS). It was found with AES that when using typical AES excitation electron-beam parameters (5 keV, 5 μA), the calcium fluoride surface decomposed, resulting in the desorption of fluorine. The ELS and XPS measurements suggest that simultaneous with the desorption of fluorine from the surface is the accumulation of calcium in a metalliclike state. Threshold measurements for the onset of fluorine desorption showed that AES analysis could be made without significant electron-beam effects by rastering a 2.5-keV, 0.05-μA electron beam over an area of 6×10^{-4} cm^2, corresponding to a current density of 0.082 mA/cm^2.

PACS numbers: 79.20.Kz

I. INTRODUCTION

Auger electron spectroscopy (AES) is a widely accepted technique for determining the elemental constituents of the outermost atomic layers of a solid. However, for certain classes of materials the analysis obtained by AES may not give an accurate composition of the surface of a material because of beam-induced effects which either can occur during the course of examination, or could have occurred almost instantaneously upon exposure to the electron beam. This electron-beam-induced damage can manifest itself not only by changes in the concentration or chemical state of surface species, but also by discoloration or physical damage of the specimen surface. A general review of electron beam damage associated with AES analysis has recently been given by Pantano and Madey.[1]

The surfaces of nonmetallic specimens are found to be particularly susceptible to electron-beam damage. The irradiation of alkali halides with electrons in the typical energy range (3–5 keV) and beam currents (5–10 μA) employed in AES have been shown to cause pronounced changes in the chemical composition of the surface.[2–6] Color centers, halogen deficiencies, and metallic aggregates have all been observed and discussed. The same holds true for fluorides, oxides, and sulphides in which color centers are produced due to the interaction of the electron beam with the surface, along with the ejection of ions and neutrals from the surface.

Calcium fluoride has been observed to decompose under electron beam impact when using typical AES beam parameters. In this paper, we report the results of our investigation of electron-beam decomposition of ion bombarded calcium fluoride surfaces using AES, electron loss spectroscopy (ELS), and x-ray photoelectron spectroscopy (XPS). AES analysis showed that this decomposition is in the form of electron-induced desorption of the fluorine. In addition, ELS and XPS measurements suggest that simultaneous with the desorption of fluorine from the surface, is the accumulation of calcium in a metalliclike state. Conditions for obtaining AES spectra from calcium fluoride under which electron-beam effects have been essentially eliminated were determined and are also reported.

II. EXPERIMENTAL

The AES and ELS studies were performed in an ion-pumped stainless steel ultrahigh vacuum (UHV) system with a base pressure of 3×10^{-8} Pa. The AES and ELS spectra were obtained using a Varian Auger spectrometer consisting of a single-pass cylindrical mirror analyzer (Model No. 981-2707) equipped with a coaxial electron gun having a maximum electron-beam energy of 10 keV and a minimum spot size of 5 μm. For the initial studies, the Auger surface analysis was performed with an electron beam energy of 5 keV and a current density of 14 mA/cm^2 (1-μA beam rastered over 7×10^{-5} cm^2). With these beam conditions, electron-beam desorption of the fluorine was observed. To reduce or eliminate electron induced desorption effects, AES spectra were obtained later using electrons at 2.5-keV energy with current densities down to 0.082 mA/cm^2. This current density was achieved by rastering a 0.05-μA beam over an area of 6×10^{-4} cm^2. In order to maintain an adequate Auger signal-to-noise level at such low beam currents, a modulation of 10 eV peak-to-peak was used for the phase-sensitive detection of the Auger current. The primary electron beam was incident at 70° with respect to the specimen normal.

The characteristic electron energy-loss spectra were obtained with the same experimental apparatus as that used for the Auger spectroscopy. Beam energies of 150, 300, and 500 eV were used to obtain ELS spectra at current densities from 40 to 120 mA/cm^2. Results were recorded using the standard ac modulation technique with a peak-to-peak modulation of 1 eV. The full-width at half-maximum (FWHM) of the elastic peak was measured to be 1.2 eV. Energy losses

[a] Present address: Monsanto Research Corporation, Mound Laboratories, Miamisburg, Ohio 45342.

 0021-8979/81/116921-07$01.10

were measured at the minima of the derivative peaks, relative to the corresponding minimum of the elastic peak.

The XPS measurements were performed in a separate vacuum system equipped with a Leybold-Heraeus LH-10 XPS spectrometer and a Mg x-ray source (1253.6 eV). In addition to XPS, this instrument contained a quadrupole mass spectrometer for residual gas analysis (RGA). Bakeout at 150 °C gave a background pressure in the low 10^{-6} Pa range.

Calcium fluoride specimens were prepared from a large grain (~ 1 cm) polycrystalline ingot supplied by the Raytheon Company, Research Division, Waltham, Massachusetts. This material was fabricated by a fusion casting process using a carbon tetrafluoride reactive atmosphere (RAP) for purification. Calcium fluoride produced by the RAP process represents the state-of-the-art in low contamination, high quality infrared optical grade material. Specimens were made by cleaving bars cut from the ingot, thereby allowing (111) surfaces with dimensions of ~ 1 cm^2 to be obtained. After bakeout, the AES spectra showed sulfur, chlorine, carbon, and oxygen as the major surface contamination as shown in Fig. 1. The specimens were argon ion sputter etched using an ion energy of 1 keV, a current density of 3 $\mu A/cm^2$, and an argon backfill pressure of 6.7×10^{-3} Pa. After 30 min of argon ion bombardment, surfaces free of sulfur, chlorine, and carbon within AES detection limits were produced [Fig. 2(a)]. Surfaces prepared in this manner will be referred to as "cleaned" calcium fluoride surfaces. The persistence of an oxygen Auger signal after argon ion sputter etching was found consistently for all of the specimens used in this study. The source of the oxygen AES signal is from oxygen contamination in the bulk of the calcium fluoride material.

III. RESULTS AND DISCUSSION

A. AES measurements

The cleaned calcium fluoride surfaces were electron bombarded using the coaxial electron gun of the Auger spectrometer. The electron beam was used both for studying its effect on the surface and for monitoring the changes in chemical composition occurring on the surface during electron bombardment. A blue glowing spot indicated the area hit by the electron beam. On removing specimens from the vacuum system, a purple coloration of the surface area impacted by the electron beam was observed. This coloration was particularly pronounced for electron beams with current densities greater than 1 mA/cm^2.

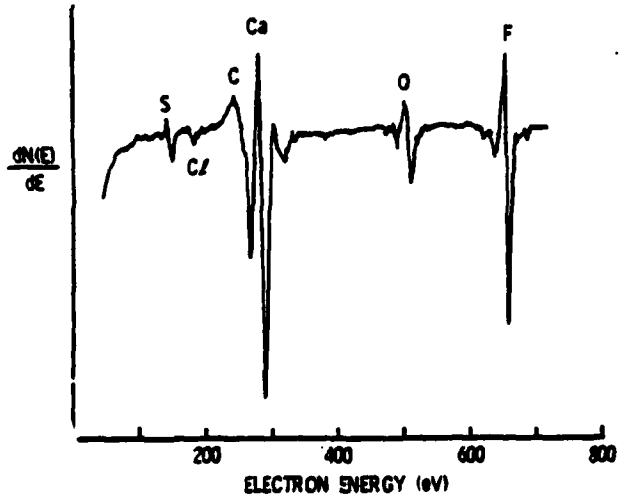

FIG. 1. Auger spectrum of an unsputtered calcium fluoride surface after bakeout of UHV system.

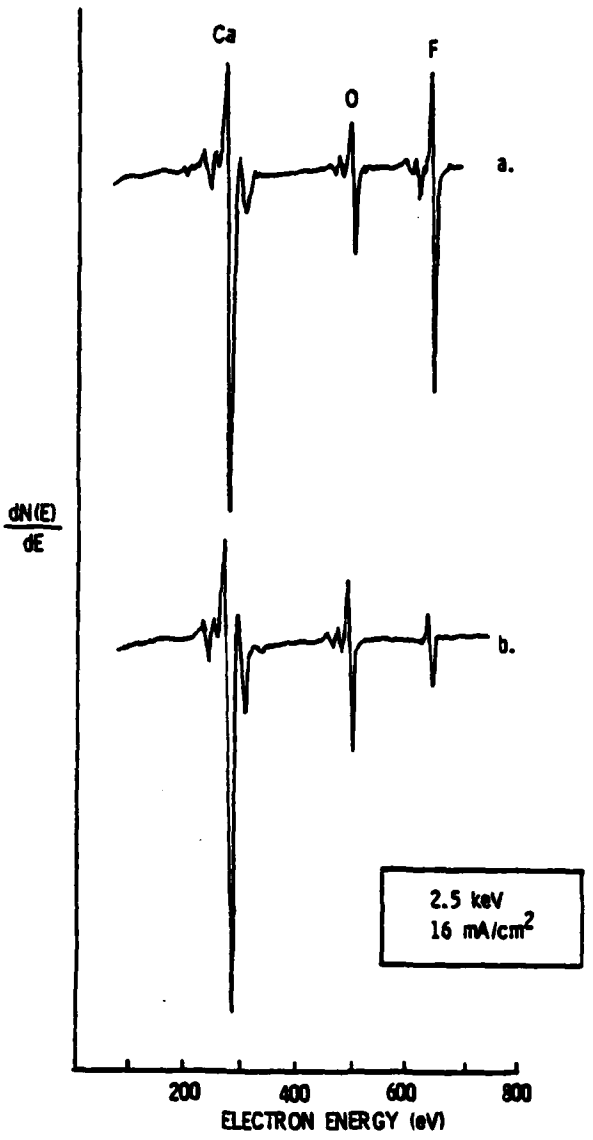

FIG. 2. Auger spectrum of a cleaned calcium fluoride surface: (a) surface after sputtering; (b) after 20 min of electron bombardment with an energy of 2.5 keV and a current density of 16 mA/cm^2. Data were taken with a 2.5-keV electron beam with a current density of 0.082 mA/cm^2.

Electron-beam-induced changes in the AES spectra of a cleaned calcium fluoride surface are shown in Fig. 2. Spectrum (a) was obtained following argon ion sputtering of the surface for 30 min using a 1-keV argon beam and a current density of 3 $\mu A/cm^2$. This typical spectrum persists for hours under UHV conditions without showing any signifi-

cant increase in concentration of carbon or oxygen contamination, provided the specimen is not decomposed by electron bombardment during that time. Spectrum (b) was obtained after exposure of the cleaned surface to an electron beam of 2.5 keV and a current density of 16 mA/cm^2 for 20 min. (The Auger analysis was done in both cases with a primary electron beam energy of 2.5 keV and a current density of 0.082 mA/cm^2 which does not produce significant decomposition of the surface—see end of this section.) It can be seen that following electron beam decomposition the relative decrease in the fluorine Auger peak-to-peak amplitude is very pronounced (4-fold decrease).

The time dependence of the Auger signal is shown in Fig. 3 using a calcium fluoride surface with a primary electron beam of 5 keV and a current density of 14 mA/cm^2. The intensity of the Auger signal was taken to be the peak-to-peak height of the dN/dE spectra. The fall-off of the fluorine Auger signal indicates that the electron beam is inducing the desorption of fluorine ions in the upper surface region of the calcium fluoride specimen.

The main Auger transitions of calcium are the $L_{2,3}MM$ transition at 293 eV and the $L_{2,3}MV$ transition at 318 eV, where the V denotes the participation of an electron from the valence band. The peak-to-peak intensity of the calcium $L_{2,3}MV$ Auger signal was observed to increase slightly during electron bombardment as shown in Fig. 3. This increase in the Auger signal of the $L_{2,3}MV$ transition of calcium can be attributed to a reduction in coordination number of the calcium ions in the surface region resulting from the loss of fluorine, thereby increasing the number of electrons associated with the valence band. On the other hand the Auger peak-to-peak intensity of the calcium $L_{2,3}MM$ transition (293 eV) remains essentially unchanged during electron bombardment. That the peak-to-peak intensity of the calcium $L_{2,3}MM$ Auger signal remains unchanged does not necessarily mean that the Auger current of the $L_{2,3}MM$ transition did not increase. It is well known that changes in the Auger line shapes can produce erroneous results when using peak-to-peak intensities as a measure of the detected Auger currents. This is found to be the case, for example, when performing AES depth profiling through thin films of aluminum and silicon oxides on their respective pure materials, in which energy shifts in the metal Auger transitions indicate a depletion of the metal near the interface in the peak-to-peak intensity depth profile.[9] Broadening of the calcium $L_{2,3}MM$ Auger peak may occur due to changes in the bonding of the calcium as a result of the loss of fluorine. Such a broadening would correspond to a higher calcium $L_{2,3}MM$ Auger current from the specimen, even though the peak-to-peak height did not change. Indeed, the calcium $2p$ levels were observed to broaden substantially after prolonged electron bombardment using XPS (see Sec. C).

Electron-beam assisted oxygen adsorption was observed depending upon the partial pressure of the oxygen containing gases (e.g., O_2, H_2O, CO, and CO_2) present in the residual gas. During electron-beam bombardment, if the partial pressure of the oxygen containing gases is below $\sim 1\times10^{-8}$ Pa, the oxygen Auger signal shows no more than perhaps a small variation in intensity. On the other hand, if the partial pressure is above $\sim 5\times10^{-8}$ Pa, the oxygen Auger signal increases simultaneously with the decrease in the fluorine Auger signal as illustrated in Fig. 4. Because of this effect, the measurements reported in this section were taken with the oxygen partial pressure less than $\sim 1\times10^{-8}$ Pa.

In order to permit Auger analysis of the calcium fluoride surface without causing electron-beam damage, a series of measurements were performed to determine the current density threshold for electron induced desorption of

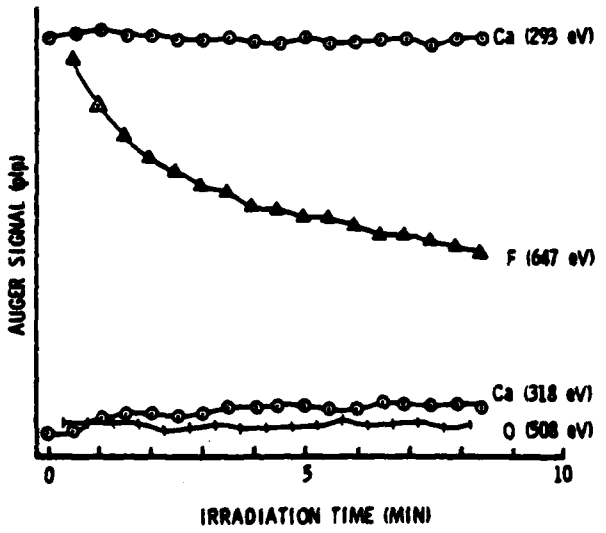

FIG. 3. Time-dependent peak-to-peak amplitude of calcium, fluorine, and oxygen Auger signals from a clean calcium fluoride surface as a function of exposure time to electron bombardment. AES signal excited by a 5-keV electron beam with a current density of 14 mA/cm^2. The partial pressures of oxygen containing residual gases are less than 1×10^{-8} Pa.

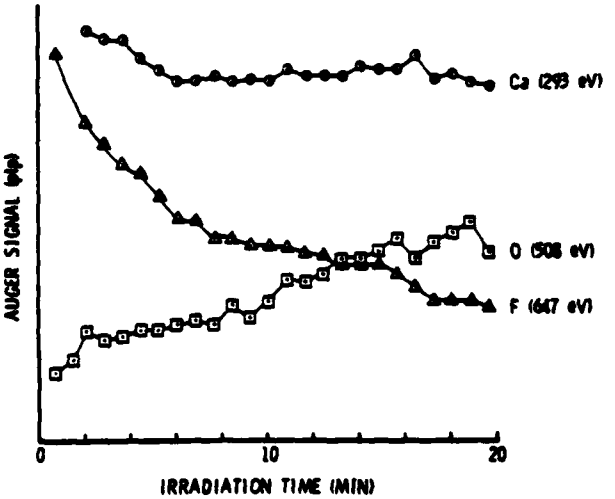

FIG. 4. Time-dependent AES peak intensities from a calcium fluoride surface as a function of exposure time to electron bombardment with a 5-keV electron beam and a current density of 14 mA/cm^2. The partial pressures of oxygen containing residual gases are above 5×10^{-8} Pa.

fluorine from the surface. Since the electron-beam diameter was not known, the current density was established by rastering the beam over an area of 6×10^{-4} cm^2. The fluorine desorption rate for a cleaned calcium fluoride surface was determined for electron-beam current densities of 0.082, 0.15, 1.6, 4.1, and 8.2 mA/cm^2.

The rate of fluorine desorption increased with increasing electron-current density. Assuming a first-order desorption process, an effective cross section for electron stimulated desorption of $\sim7.5\times10^{-19}$ cm^2 was determined for a 2.5-keV electron beam from the fluorine Auger signal strength taken as a function of electron irradiation time. Using this cross section leads to a calculated damage threshold or critical electron dose D_d of ~0.21 C/cm^2, assuming a 10% detectable change in concentration of fluorine within the expected escape depth of nine monolayers. This electron dose can be related to the electron beam parameters since electron dose is given by the product of current density (amps/cm^2) and time (sec). Hence, on the basis of the value given above for D_d, detectable damage to a calcium fluoride surface would not occur until 35 min for an electron current density of 0.1 mA/cm^2. Indeed, for current densities of 0.16 mA/cm^2 and below, little variation in the magnitude of the fluorine Auger signal was observed for exposures up to 20 min as illustrated in Fig. 5.

There are two mechanisms by which an electron beam can cause a color center and the dissociation of a fluorine atom from the surface. One possible mechanism is the absorption of electrons with low energy ($\sim$2–4 eV) in the valence band leading to a chemical dissociation process analogous to the process proposed by Hersh[10] and by Pooley[11] for the formation of color centers in alkali halides. Another possible mechanism is that recently proposed by Knotek and Feibelman[12] which in particular should be applicable to ionic solids. As suggested by these authors the probable path to desorption is that in a maximal valency ionic compound, such as calcium fluoride, an interior intra-atomic Auger decay of the core holes produced by the electron beam leads to a removal of two (or even three) electrons from the anions. This will make the Madelung potential, which is strongly attractive in the ground state, strongly repulsive and thus lead to desorption of neutral or positively charged ions. In the case of calcium fluoride, such a mechanism is feasible via an intra-atomic Auger transition originating from a fluorine 2s hole. However, the desorption data presented here does not clarify which mechanism is operative for the electron beam-induced desorption of fluorine from calcium fluoride.

From the Auger measurements it was noted that when a calcium fluoride surface is exposed to an electron beam with current densities greater than 0.16 mA/cm^2, a pronounced decrease in the fluorine Auger signal strength is observed. On the other hand a small increase in the calcium $L_{2,3}MV$ is observed while little change in the calcium $L_{2,3}MM$ Auger signal is noted. To characterize the chemical changes undergone by the calcium ions during electron beam bombardment, studies of electron irradiated calcium fluoride surfaces were performed using ELS and a combination of XPS and x-ray stimulated AES (XAES). The following two sections describe the results of these studies.

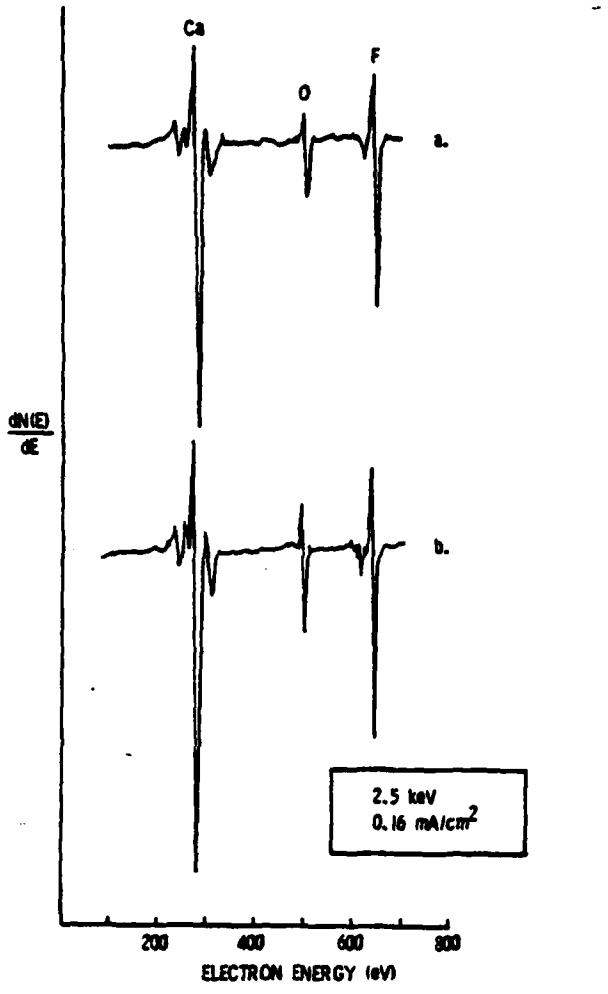

FIG. 5. Auger spectrum of a clean calcium fluoride surface: (a) before electron bombardment; (b) after 20 min of exposure to an electron beam with an energy of 2.5 keV and a current density of 0.16 mA/cm^2.

B. Electron-loss measurements

Electron-loss measurements of air cleaved calcium fluoride surfaces at room temperature were made using incident electron-beam energies of 150, 300, and 500 eV at current densities from 40 to 120 mA/cm^2. A series of energy-loss spectra taken as a function of irradiation time for an incident electron energy of 150 eV are shown in Fig. 6. Loss peaks were observed at 3, 7, 11, 15, 27, and 33 eV below the elastic peak. The electron loss spectra obtained with the 300- and 500-eV incident electron beam were found to be similar to those obtained in the 150-eV beam studies.

As shown in Fig. 6, the accumulative electron-beam bombardment of the calcium fluoride surface produced significant changes in the energy-loss spectrum. In each of the ELS spectra the two lowest energy-loss peaks are enhanced in intensity with increasing irradiation time. Simultaneous with the increase in these peaks, the loss peak at 15 eV is gradually obliterated.

Based on experimental loss data[13] and electronic energy band calculations,[14] reasonable assignments can be made to

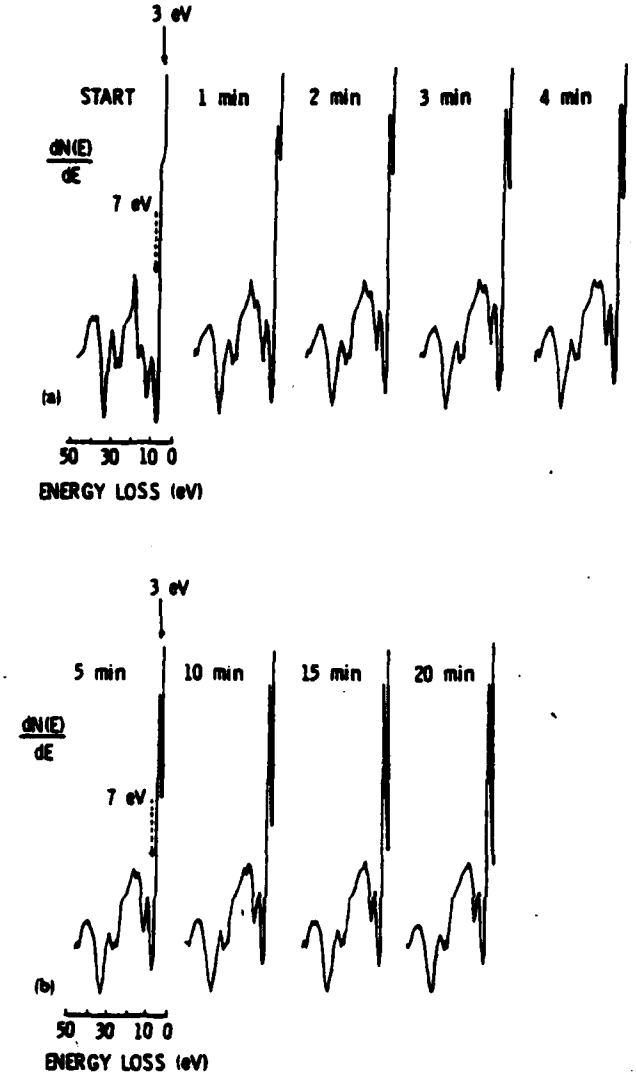

FIG. 6. Energy-loss spectra of an air cleaved calcium fluoride surface excited with a 150-eV electron beam with increasing time of irradiation. (a) Initial sequence of ELS spectra, (b) final time sequence showing the increase in the 3-eV loss peak.

the observed electron-loss spectra. Table I lists the energy losses of the calcium fluoride surface taken at a primary electron energy of 150 eV. Also listed in the table are the energy-loss values found from electron transmission measurements[13] and from optical measurements.[15] Further, a labeling and proposed origin for each loss peak is also given.

The strong 33-eV loss is caused by electronic transitions from the low valence bands originating mainly from the $3p$ Ca^{++} orbitals, $\Gamma_{15}(p^+)$, to high conduction bands. The loss at 27 eV is attributed to the core exciton transition $\Gamma_{15}(p^+) \rightarrow \Gamma_1$. The structure at 11 and 15 eV corresponds to resonant excitons associated with the allowed $\Gamma_{15} \rightarrow \Gamma_1$ and $X'_5 \rightarrow X_3$ transitions, respectively.

The origins of the loss peaks at 3 and 7 eV are not as easily assigned. From the AES results and visual examination of the damaged surface, the electron beam not only induces the desorption of fluorine from the calcium fluoride

TABLE I. Values of the energy-loss peak observed for calcium fluoride.

Characteristic losses (eV): Present work	Electron transmission [a]	Optical reflection [b]	Energy-losses designation
3			F-centers[c]/Ep_s(Ca)[d]
7			Ep_b(Ca)[d]
11	11.8	11.18	$\Gamma_{15}(p^-) \rightarrow \Gamma_1$ exciton
15	15.8	15.4	$X'_5(p^-) \rightarrow X_3$ exciton
27	27.9	27.7	$\Gamma_{15}(p^+) \rightarrow \Gamma_1$ core exciton
33	33.6	32.8–34.5	$\Gamma_{15}(p^+) \rightarrow \Gamma'_{25}, \Gamma_{12}$

[a] Ref. 13.
[b] Ref. 15.
[c] Ref. 17.
[d] Ref. 18.

surface but also causes a purple coloration of the surface area exposed by the electron beam. This coloration of the surface is indicative of the formation of color centers (F-center), which are electron-containing fluorine ion vacancies. Both theoretical calculations[16] as well as optical absorption measurements[17] show that the optical transition energy of an F-center in calcium fluoride is 3.3 eV. This transition energy agrees with the observed low-energy-loss peak at 3 eV. Furthermore, the behavior of the 3-eV loss peak with increasing exposure of the calcium fluoride surface to high current density electron-beam impact is typical of that expected for the increase in concentration of F-centers as time progresses. In addition, the gradual obliteration of the 15-eV loss peak concurrent with the increase in the 3-eV peak is consistent with the formation of fluorine vacancies, since the excitonic transition at 15 eV originates from the valence band composed of $p\,F^-$ orbitals. However, color center formation does not explain the origin and behavior of the loss peak at 7 eV.

An alternative explanation, consistent with the observed ELS data, is that in addition to the formation of fluorine vacancies, the electron beam also causes the formation of calcium atoms in a metal-like state. Electron-loss data have been reported for calcium metal by Robins and Best.[18] They noted loss peaks at 3.4, 8.8, 12.5, 27.4, 36.9, and 45.6 eV. The peaks at 27.4 and 45.6 eV were assigned to electronic transitions involving $3p$ and $3s$ metal electrons which have been promoted to states above the Fermi level. The highest intensity loss peaks observed by Robins and Best at 3.4 and 8.8 eV were assigned to surface and bulk plasmon excitations, respectively. The 12.5-eV loss was attributed to the combination of the surface and bulk plasmon loss.

The ELS data of Robins and Best for calcium metal indicates that the 3- and 7-eV loss peaks observed for electron decomposed calcium fluoride could result from surface and bulk plasmon excitations of calcium in a metallic-like state formed following the electron induced desorption of fluorine from the surface. In addition, the fact that the loss peak at 11 eV, which for calcium fluoride originates also from the $p\,F^-$ valence band, does not decrease with electron bombardment, but remains constant and perhaps increases slightly, indicates that color center formation is not the only possible chemical change occurring at the surface during electron impact.

C. X-ray photoelectron measurements

In this section results on electron-beam decomposition of cleaved calcium fluoride using a combination of XPS and XAES are presented. The study involved XPS and XAES measurements on the surface chemistry before electron bombardment and following electron bombardment by a 5-keV electron beam with a current density of about 0.2 mA/cm^2. After two hours of electron bombardment at this current density, the fluorine XPS and XAES integrated intensities were reduced by about 64% of their original intensities as shown in Figs. 7(a) and 7(b), respectively.

The change in the chemical state of the calcium ions before and after electron bombardment is shown in Figs. 8 and 9. Figure 8 presents the XAES spectrum for the calcium $L_{2,3}MM$ Auger electron lines. A comparison of the two spectra shows that the electron beam damage resulted in a shift in the Auger lines by about 6 eV. In addition, it is seen that the intensities of the two predominant Auger transitions before and after electron irradiation are interchanged. However, the most pronounced effect of the electron impact is reflected in the calcium $2p$ photoemission spectra. As shown in Fig. 9, the calcium $2p$ photoemission lines split into a second set of $2p$ photoemission lines at 2.4 eV lower in binding energy.

Along with the splitting of the calcium $2p$ photoemission line was an increase in the oxygen $1s$ photoemission peak as shown in Fig. 10. The oxygen $1s$ photoelectron peak which is shifted to a higher binding energy following electron irradiation, is characteristic of adsorbed oxygen rather than a native oxide.[19,20] Throughout this study, the observed carbon $1s$ photoelectron signal indicated that carbon was present at a level of less than 1 at. % on the calcium fluoride surface.

We attribute the chemically shifted calcium $2p$ photoelectron peaks to lower binding energies to calcium ions in and near the surface which have undergone a reduction in coordination number because of the desorption of fluorine by the stimulus of the electron beam. Since the oxygen $1s$ photoelectron peak was observed to increase in intensity after electron irradiation, part of the shift in the calcium $2p$

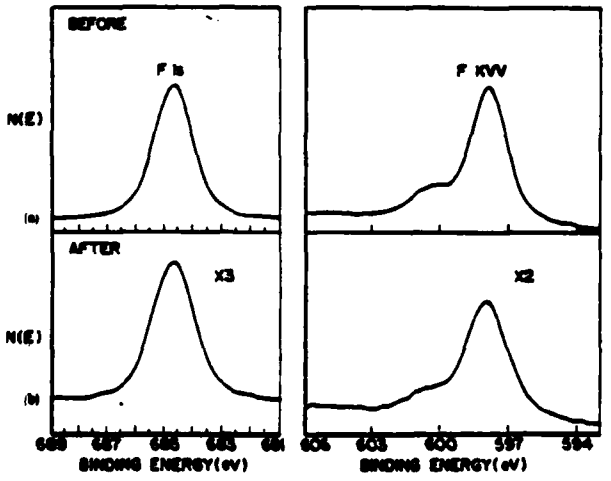

FIG. 7. Fluorine signal of a cleaved calcium fluoride surface before and after two hours of electron bombardment with a 5-keV electron beam with a current density of 0.2 mA/cm^2. (a) the XPS spectrum of the fluorine $1s$ photoemission line; (b) the XAES spectrum of the fluorine KVV Auger transition.

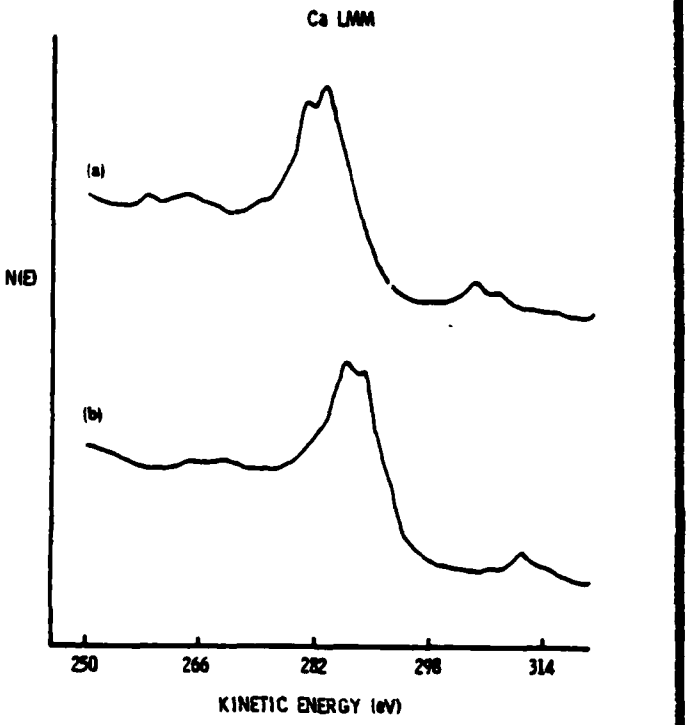

FIG. 8. X-ray stimulated AES spectrum of a cleaved calcium fluoride surface showing the calcium LMM Auger transition: (a) before electron-beam bombardment; (b) after two hours of electron bombardment with a 5-keV electron beam with a current density of 0.2 mA/cm^2.

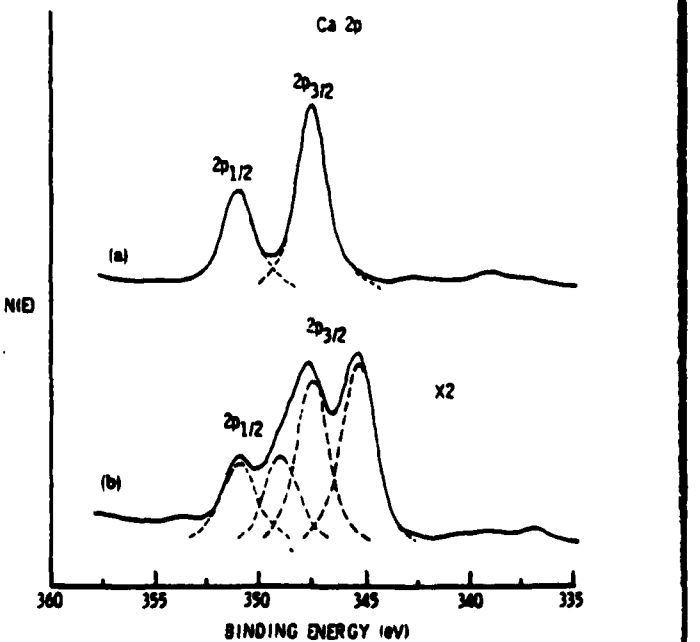

FIG. 9. XPS spectrum of a cleaved calcium fluoride surface showing the calcium $2p$ photoemission lines: (a) before electron-beam bombardment; (b) after two hours of electron bombardment with a 5-keV electron beam at 0.2 mA/cm^2.

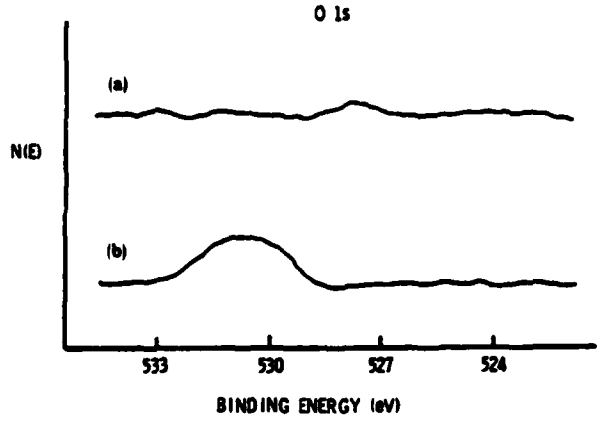

FIG. 10. XPS spectrum of a cleaved calcium fluoride surface showing the oxygen 1s photoemission line: (a) before electron-beam bombardment; (b) after two hours of electron bombardment with a 5-keV electron beam at 0.2 mA/cm^2.

photoemission lines may be associated with the reaction of oxygen atoms in the residual gas with the fluorine vacancies generated by the electron beam.

However, when the calcium $2p$ photoelectron binding energy is referred to the fluorine $1s$ peak position (684.7 eV as measured by Wagner *et al.*[21] for calcium fluoride), the binding energy for the shifted calcium $2p_{3/2}$ photoemission peak is determined to be 345.2 eV. This value is in good agreement with the calcium $2p_{3/2}$ binding energy measured by Van Doveren and Verhoeven[22] for calcium metal (345.7 eV). Furthermore, the calcium $2p_{3/2}$ photoelectron peak assigned to calcium fluoride has a binding energy which is within 0.2 eV of that reported by Wagner[23] (347.7 eV).

IV. CONCLUSIONS

The interaction of electron beams with cleaned surfaces of calcium fluoride was monitored by AES, ELS, and XPS. The results presented show that the bombarding electrons can cause decomposition of the surface. This decomposition is in the form of electron-induced desorption of fluorine and a simultaneous accumulation of fluorine vacancies (color centers) and metalliclike calcium on the surface. The electron damaged calcium fluoride surface was found to be particularly sensitive to oxygen and may be oxidized by residual gas phase components.

The rate of fluorine desorption was found to be dependent upon the current density of the incident electron beam. From this work, it was found that AES measurements could be made without producing significant electron beam decomposition by rastering a 2.5-keV electron beam over a area of 6×10^{-4} cm^2 using a current density of 0.16 mA/cm^2 or less.

ACKNOWLEDGMENTS

The authors wish to thank T. Wittberg and J. Hoenigman for useful discussions. We also acknowledge support for this research from the United States Air Force Office of Scientific Research under Grant No. 78-3666.

[1]C. G. Pantano and T. E. Madey, Appl. Surf. Sci. 7, 115 (1981).
[2]P. D. Townsend and J. C. Kelly, Phys. Lett. A 25, 673 (1967).
[3]P. D. Townsend and J. C. Kelly, Phys. Lett. A 26, 138 (1968).
[4]P. W. Palmberg and T. N. Rhodin, J. Phys. Chem. Solids 29, 1917 (1968).
[5]H. Tokutaka, M. Prutton, I. G. Higginbotham, and T. E. Gallon, Surf. Sci. 21, 233 (1970).
[6]I. G. Higginbotham, T. E. Gallon, M. Prutton, and H. Tokutaka, Surf. Sci. 21, 241 (1970).
[7]L. S. Cota Araiza and B. D. Powell, Surf. Sci. 51, 504 (1975).
[8]A. Friedenberg and Y. Shapira, Surf. Sci. 87, 581 (1979).
[9]J. T. Grant, R. G. Wolfe, and M. P. Hooker, J. Vac. Sci. Technol. 14, 232 (1977).
[10]H. N. Hersch, Phys. Rev. 148, 928 (1966).
[11]D. Pooley, Proc. Phys. Soc. London 87, 245 (1966).
[12]M. L. Knotek and P. J. Feibelman, Surf. Sci. 90, 78 (1979).
[13]J. Frandon, B. Lahaye, and F. Pradal, Phys. Status Solidi 53, 565 (1972).
[14]J. P. Albert, C. Jouanin, and C. Gout, Phys. Rev. B 16, 4619 (1977).
[15]G. W. Rubloff, Phys. Rev. B 5, 662 (1972).
[16]H. S. Bennett, Phys. Rev. B 3, 2763 (1971).
[17]B. C. Cavanett, W. Hayes, I. C. Hunter, and A. M. Stoneham, Proc. Roy. Soc. London A 309, 53 (1969).
[18]J. L. Robins and P. E. Best, Proc. Phys. Soc. London 79, 110 (1962).
[19]T. Robert, M. Bartel, and G. Offergeld, Surf. Sci. 33, 123 (1972).
[20]J. C. Fuggle, L. M. Watson, D. J. Fabian, and S. Affrossman, Surf. Sci. 49, 61 (1975).
[21]C. D. Wagner, L. H. Gale, and R. H. Raymond, Anal. Chem. 51, 466 (1979).
[22]H. van Doveren and J. A. TH. Verhoeven, J. Electron Spectrosc. Relat. Phenom. 21, 265 (1980).
[23]C. D. Wagner, Discuss. Faraday Soc. 60, 291 (1975).

APPENDIX B

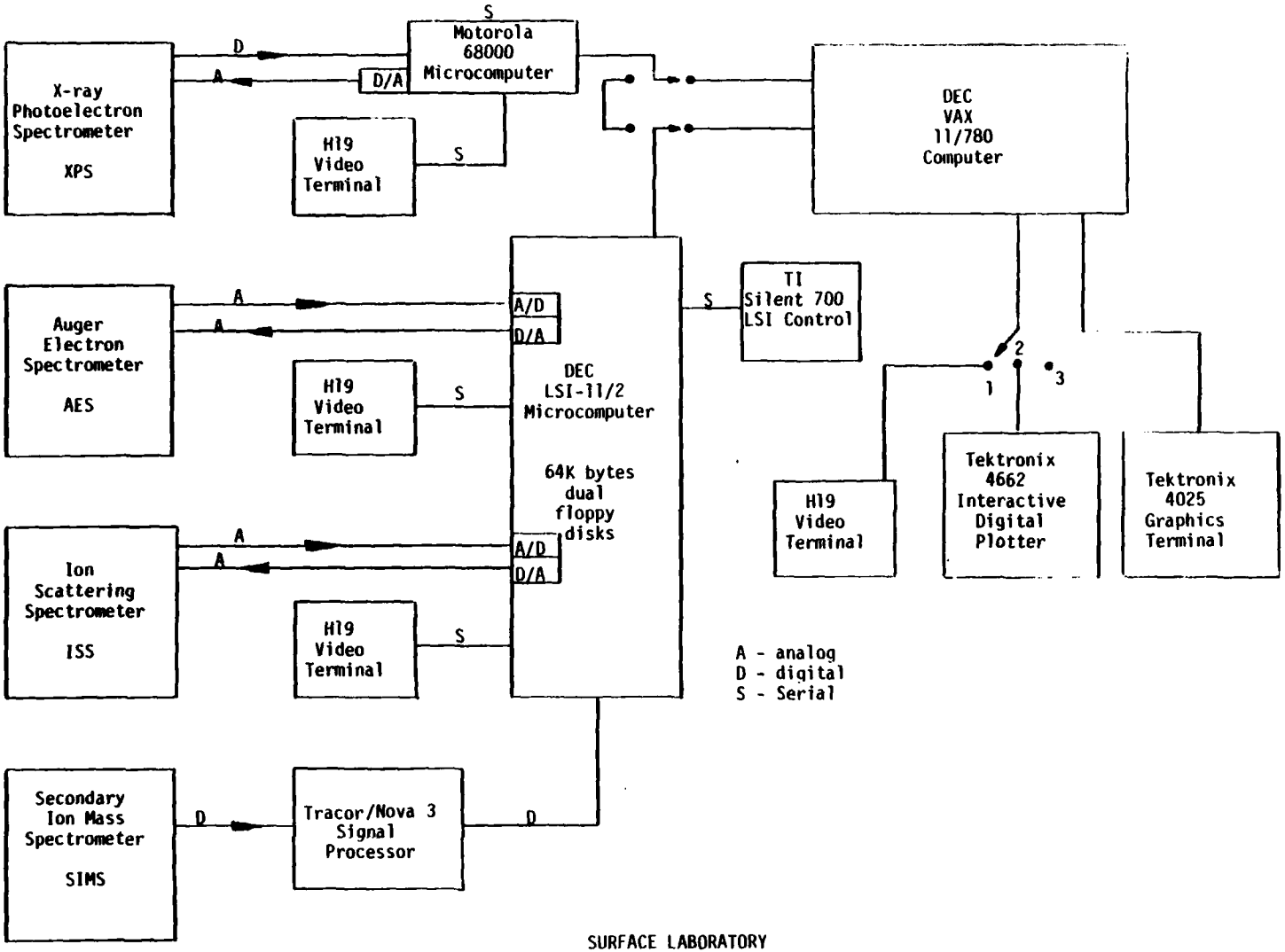

SURFACE LABORATORY

Automated Data Acquisition and Analysis System.